DISSERTATIONES
CHIMICAE
UNIVERSITATIS
TARTUENSIS
207

SIMONA SELBERG

Development of Small-Molecule Regulators of Epitranscriptomic Processes

DISSERTATIONES CHIMICAE UNIVERSITATIS TARTUENSIS
207

DISSERTATIONES CHIMICAE UNIVERSITATIS TARTUENSIS
207

SIMONA SELBERG

Development of Small-Molecule Regulators of Epitranscriptomic Processes

UNIVERSITY OF TARTU
Press

Institute of Chemistry, Faculty of Science and Technology, University of Tartu, Estonia

Dissertation is accepted for the commencement of the degree of *Doctor philosophiae* in Chemistry on June 18th, 2021 by the Council of Institute of Chemistry, Faculty of Science and Technology, University of Tartu

Supervisor: Prof. Mati Karelson (PhD)
Institute of Chemistry, University of Tartu, Estonia

Opponent: Anna Kula-Păcurar (PhD), Assistant Professor
Malopolska Centre of Biotechnology,
Jagiellonian University Krakow, Poland

Commencement: September 3rd, 2021, 12.15
Ravila Street 14a, Tartu (Chemicum), auditorium 1020

This work has been partially supported by Graduate School of Functional materials and technologies receiving funding from the European Regional Development Fund in University of Tartu, Estonia.

ISSN 1406-0299
ISBN 978-9949-03-665-3 (print)
ISBN 978-9949-03-666-0 (pdf)

University of Tartu Press
www.tyk.ee

TABLE OF CONTENTS

LIST OF ORIGINAL PUBLICATIONS

I. Selberg, S.; Blokhina, D.; Aatonen, M.; Koivisto, P.; Siltanen, A.; Mervaala, E.; Kankuri, E.; Karelson, M. Discovery of Small Molecules that Activate RNA Methylation through Cooperative Binding to the METTL3-14-WTAP Complex Active Site. *Cell Reports* **2019**, 26 (13), 3762–3771, DOI: 10.1016/j.celrep.2019.02.100.

II. Selberg, S.; Yu, L.-Y.; Bondarenko, O.; Kankuri, E.; Seli, N.; Kovaleva, V.; Herodes, K.; Saarma, M.; Karelson, M. Small-Molecule Inhibitors of the RNA m^6A Demethylases FTO Potently Support the Survival of Dopamine Neurons. *International Journal of Molecular Sciences* **2021**, 22 (9), 4537, DOI: 10.3390/ijms22094537.

III. Selberg, S.; Seli, N.; Kankuri, E.; Karelson, M. Selberg, S.; Seli, N.; Kankuri, E.; Karelson, M. Rational Design of Novel Anticancer Small-Molecule RNA m6A Demethylase ALKBH5 Inhibitors. *ACS Omega* **2021**, 6 (20), 13310–13320, DOI: 10.1021/ acsomega. 1c01289.

IV. Selberg, S.; Žusinaite, E.; Herodes, K.; Seli, N.; Kankuri, E.; Merits, A.; Karelson, M. HIV replication is increased by RNA methylation METTL3/ METTL14/WTAP complex activators. *ACS Omega* **2021**, 6 (24), 15957–15963, DOI: 10.1021/acsomega.1c01626.

Author´s contribution

Paper I. Lead author in preparing the manuscript. Performed all computational modelling and virtual screening, some of the measurement experiments.

Paper II. Lead author in preparing the manuscript. Performed all computational modelling and virtual screening and some of the measurement experiments.

Paper III. Lead author in preparing the manuscript. Performed all computational modelling and virtual screening and most of the experimental measurements.

Paper IV. Lead author in preparing the manuscript. Performed most of the experimental measurements.

ABBREVIATIONS

6-OHDA	6-hydroxydopamine
ALKBH3	α-ketoglutarate-dependent dioxygenase AlkB homolog protein 3
ALKBH5	α-ketoglutarate-dependent dioxygenase AlkB homolog protein 5
ALKBH9	α-ketoglutarate-dependent dioxygenase AlkB homolog proteins 9
AML	acute myeloid leukemia
B3LYP	Becke, 3-parameter, Lee–Yang–Parr
BLI	bio-layer interferometry
DARTS	drug affinity responsive target stability
DNA	*deoxyribonucleic acid*
EC_{50}	half maximal effective concentration
FIMM	Functional molecular IMMunology
FOXM1	forkhead box protein M1
FTO	fat mass and obesity-associate protein
GDNF	glial cell line-derived neurotrophic factor
HIV-1	human immunodeficiency virus type 1
HNRNPA2B1	heterogeneous nuclear ribonucleoprotein A2/B1
HTVS	high-throughput virtual screening
IC_{50}	half maximal inhibitory concentration
IGF2BP1	insulin like growth factor 2 MRNA binding protein 1
IGF2BP2	insulin like growth factor 2 MRNA binding protein 2
IGF2BP3	insulin like growth factor 2 MRNA binding protein 3
K_D	dissociation constant
KIAA1429	protein virilizer homolog
LE	ligand efficiency
m^1A	N^1-methyladenosine
m^3U	^{3}-methyluracil
m^3T	^{3}-methylthymidine
m^6A	N^6-methyladenosine
m^6A_m	N^6,2'-O-dimethyladenosine
MAT2A	methionine adenosyltransferase 2A
METTL3	methyltransferase-like protein 3
METTL14	methyltransferase-like protein 14
METTL16	methyltransferase-like protein 16
mRNA	messenger RNA
MST	microscale thermophoresis
OPLS	optimized potentials for liquid simulations
p24	viral capsid p24 protein
PDB	Protein DataBank
PMA	phorbol-12-myristate-13-acetate

RBM15	RNA-binding motif protein 15
RMSD	root mean square deviation
RNA	ribonucleic acid
rRNA	ribosomal RNA
SAH	S-adenosyl-L-homocystein
SAM	S-adenosyl-L-methionine
SPR	surface plasmon resonance
tRNA	transport RNA
U6 snRNA	U6 spliceosomal RNA
VIRMA	protein virilizer homolog
WTAP	Wilms' tumor 1-associating protein
YTHDC1	YTH domain-containing protein 1
YTHDC2	YTH domain-containing protein 2
YTHDF1	YTH N^6-methyladenosine RNA binding protein 1
YTHDF2	YTH N^6-methyladenosine RNA binding protein 2
YTHDF3	YTH N^6-methyladenosine RNA binding protein 3
ZC3H13	zinc finger CCCH domain-containing protein 13

INTRODUCTION

DNA methylation, histone modifications, gene expression regulation mediated by non-coding RNAs and chromatin remodeling are the classic epigenetic mechanisms. During the last decade, there has been a growing interest in various chemical modifications to both coding and noncoding RNAs. Such modifications with different functional groups have emerged as key mechanisms in the body to control gene expression. This area of research is called epitranscriptomics. The most common RNA modification is the methylation at the sixth position of adenosine, N^6-methyladenosine (m^6A). It affects splicing, intracellular distribution, translation, and cytoplasmic degradation of RNA. Hence, m^6A plays a crucial role in regulating cell differentiation, neuronal signaling, immune tolerance, carcinogenesis and other, both physiological and pathological, conditions. The proteins that regulate the abundance and downstream effects of RNA m^6A are known as RNA m^6A methyltransferases, RNA m^6A demethylases and RNA m^6A reader proteins. The m^6A methyltransferases and demethylases are enzymes that catalyze the transfer or removal of the methyl group from the 6^{th} position of adenosine and are therefore viable to the reversible regulation by small-molecule inhibitors and/or activators. Development of new drugs based on identification of first lead candidates holds great potential for treatment of various pathologies. As a therapeutic approach, this has attracted great interest but depends on the type of disruption in m^6A homeostasis.

The aim of this study was to carry out computational molecular design of small-molecule inhibitors and activators of enzymes involved in the regulation of RNA m^6A methylation and demethylation. Specifically, those included the RNA m^6A methyltransferase complex METTL3/METTL14/ WTAP and the RNA m^6A demethylases FTO and ALKBH5. The inhibitory or activating activity of the compounds was tested experimentally using the relevant enzymatic assays. Furthermore, the activity of these compounds was studied in various *in vitro* models related to different pathologies such as neurodegeneration, cancer and human immunodeficiency virus type 1 (HIV-1) virus infection.

1. LITERATURE OVERVIEW

1.1. RNA m^6A regulation

Today, regenerative therapies are expected to deliver their promise of fully functional tissue repair through reversible epigenetic regulation of gene expression in tissues. Epigenetics is a field of research that investigates how changes in gene expression are passed on to progeny without alterations in the DNA sequence. Epigenetic modifications include DNA methylation, histone modification, chromatin modification, and regulation of non-coding RNA. [1] The field of the study of the chemically modified RNAs and their role in physiological and pathological processes is called *epitranscriptomics*. Presently, more than 160 different post-transcriptional chemical modifications have been identified in RNA molecules [2]. The most common RNA modification is N^6-methyladenosine (m^6A). In different types of RNAs, for example messenger RNAs (mRNAs), transfer RNAs (tRNAs), ribosomal RNAs (rRNAs), m^6A is one of the most important post-transcriptional regulatory markers. Additionally, RNA m^6A modifications have an important role in the regulation of RNA splicing, translation, stability and translocation. [1, 3–5] The m^6A modifications account for about 50% of the total number of methylated ribonucleotides, and 0.1-0.4% of all adenosines in cellular RNA are methylated at the sixth position of nitrogen atoms [2].

The homeostasis of RNA m^6A modifications in cells is affected by various enzymes. RNA adenosine methylation is carried out by enzymes called m^6A *methyltransferases* and demethylation is performed by m^6A *demethylases*. Therefore, m^6A is considered to be a reversible RNA modification [6–8]. In addition, the fate of the m^6A modified RNAs in the cell is controlled by specific m^6A-binding proteins called m^6A *readers*. [1, 4, 9]

1.2. RNA m^6A methylation

As described above, the methylation of RNA at the sixth position of adenosine is performed by enzymes or enzyme complexes called RNA m^6A methyltransferases, also known as *writers* [9]. In cells, the methyl group is added to adenosine mainly by the methyltransferase complex involving methyltransferase-like protein 3 (METTL3) and methyltransferase-like protein 14 (METTL14). This METTL3/METTL14 complex is generally bound to auxiliary proteins such as the Wilms' tumor 1-associating protein (WTAP) [10–12], protein virilizer homolog (KIAA1429 or VIRMA) [13], RNA-binding motif protein 15 (RBM15) [14] or zinc finger CCCH domain-containing protein 13 (ZC3H13) [15]. Another m^6A methylating enzyme in cells is the methyltransferase-like protein 16 (METTL16) [16]. Of all these proteins, the 3D crystal structure is known only for METTL3/METTL14 [17–20] heterodimer and METTL16 [21–24] enzyme. These methyltransferases are predominantly

located in the cell nucleus where the methylation is also performed [25]. Chemically, RNA m^6A methyltransferases catalyze the methyl group transition from S-adenosyl-L-methionine (SAM) molecule to adenosine in RNAs (Figure 1).

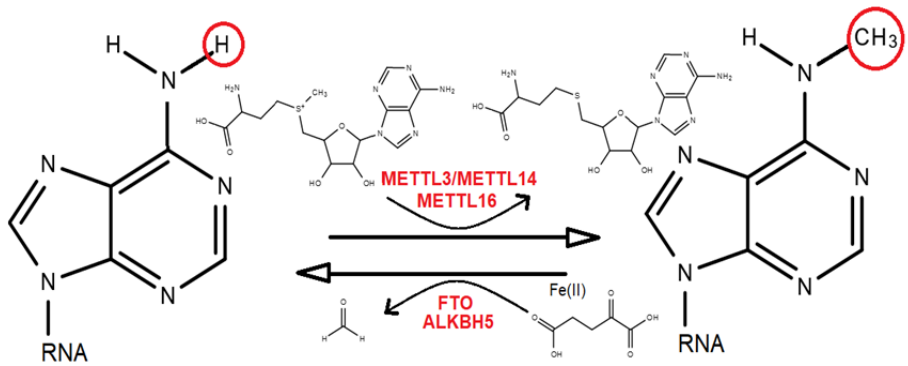

Figure 1. Reversible m^6A methylation in RNA [26].

The products of this enzymatic reaction are m^6A-methylated RNA and S-adenosyl-L-homocysteine (SAH). [20, 26]

The RNA methyltransferase METTL3/METTL14/WTAP complex is one of the most common RNA m^6A methyltransferases and therefore we chose it as the object of study in this work. METTL3 is highly conserved in indigenous organisms from yeast to humans [10]. Another component of the complex is METTL3 protein homologue METTL14 that co-localizes with METTL3 as a stable heterocomplex [11, 27]. The METTL3 and METTL14 enzymes have a main catalytic role in the addition of methyl group to RNA adenosine. The catalytic center is localized in METTL3 enzyme, while METTL14 enzyme assists METTL3 to recognize the substrate RNA and provides structural support for stabilizing the methylation complex [1, 13]. The WTAP protein binds to the METTL3 and METTL14 enzymes and is required for localization of the complex to nuclear speckles [28]. The function of the WTAP protein is to control the methylation process [20]. Recently, the 3D crystal structure of another RNA methyltransferase was identified. This enzyme is METTL16 [23], which is a homologue of METTL3. METTL16 methylates two substrates: U6 spliceosomal RNA (U6 snRNA) and methionine adenosyltransferase 2A (MAT2A) gene of mRNA [16, 29, 30].

No active inhibitors have yet been found for most RNA m^6A methyltransferases. Two papers describing METTL3 enzyme inhibitors have recently been published. Yankova et al. describe the best inhibitor with the half maximal inhibitory concentration (IC_{50}) of 16.9 nM and the activity of inhibitors described by Bedi et al. remain on the micromolar scale. [18, 19]

1.3. RNA m^6A demethylation

Proteins involved in the demethylation of RNA N^6-methyladenosine are called RNA m^6A demethylases or *erasers* [9]. The two best known demethylases are the fat mass and obesity-associate protein (FTO) and α-ketoglutarate-dependent dioxygenase AlkB Homolog protein 5 (ALKBH5) [31, 32]. 3D crystal structures are also known for both proteins [32–41]. Recently, the α-ketoglutarate-dependent dioxygenase AlkB Homolog protein 3 (ALKBH3) has been discovered to bind to m^6A of tRNA and the activity of other proteins of the AlkB family are also expected to behave like demethylases [42]. Similar to methyltransferases, demethylase proteins are located both in the cell nucleus [25] and cytoplasm [43].The RNA m^6A demethylation reaction is performed in the presence of Fe(II+) ion and α-ketoglutarate (Figure 1) [20].

The most investigated RNA m^6A demethylase is the FTO enzyme. FTO has been also identified as α-ketoglutarate-dependent dioxygenase AlkB Homolog protein 9 (ALKBH9) [44]. The FTO enzyme can demethylate single-stranded DNA and RNA at m^6A. In addition, FTO can demethylate N^6,2'-O-dimethyladenosine (m^6A_m), N^1-methyladenosine (m^1A) and 3-methyluracil (m^3U) and/or 3-methylthymidine (m^3T) but enzymatic activity in these processes is significantly less efficient than the demethylation of m^6A [45–48]. Another RNA m^6A demethylase, ALKBH5, has also been studied extensively. Like FTO enzyme, the ALKBH5 enzyme demethylates single-stranded DNA and RNA at m^6A. It has been suggested that ALKBH5 enzyme is more specific for m^6A than FTO [46]. Some non-specific FTO inhibitors have been reported in the literature, with their IC_{50} values in the micromolar range [32, 34, 49–52]. The best known FTO inhibitor is the cancer drug candidate Bisantrene with activity at the high nanomolar to low micromolar range [53]. Recently, an inhibitor of the ALKBH5 with IC_{50} approximately at 25 μM has been identified [54].

1.4. RNA m^6A reader proteins

In addition to methyltransferases and demethylases, another type of proteins is related to RNA m^6A modification, the RNA m^6A readers. Readers are proteins that recognize a m^6A modification in mRNA and regulate gene expression in several ways depending on the presence and location of it in the RNA [55, 56]. A group of RNA m^6A reader proteins belong to the members of the YTH domain family. These include YTH N^6-methyladenosine RNA binding proteins (YTHDF1, YTHDF2, YTHDF3) [57] and YTH domain-containing proteins (YTHDC1, YTHDC2) [58]. In addition, insulin like growth factor 2 mRNA binding proteins (IGF2BP1, IGF2BP2 and IGF2BP3) [59] and heterogeneous nuclear ribonucleoprotein A2/B1 (HNRNPA2B1) [60] are considered also as m^6A readers. The reader proteins are located in both the nucleus and the cytoplasm [1]. The 3D crystal structures for all proteins in the YTH domain family and other reader proteins have been reported [61–76]. Nevertheless, no inhibitors have yet been found for any of the reader proteins.

1.5. The role of RNA m^6A modification in physiology and pathology

RNA m^6A methylation and demethylation are reversible processes [8]. The dynamic homeostasis of m^6A methylation in critical for cellular physiological processes including cell proliferation, differentiation, metabolism, and death [7]. The abundance of RNA m^6A modification is associated with the control of cell fate decisions of stem cells and also somatic cells [77–81]. The m^6A modification of RNA is critical for the development and functions of several tissues like brain, liver or kidney. In addition to physiological processes, the RNA m^6A modification has also been associated with a number of pathologies such as developmental disorders, immunological disorders, diabetes, different types of cancer, cardiovascular diseases, neuronal diseases and infectious diseases [79].

The m^6A modifications in both the viral RNA and host cell mRNAs play critical role in virus genome transcription and virus replication. The presence of m^6A modifications in viral RNA has been observed in many viruses such as HIV, herpes simplex virus, hepatitis B virus, Zika virus, influenza A virus and other RNA viruses. [82–90] The occurrence of m^6A in viral RNA regulates virus replication and gene expression as demonstrated in the case of HIV-1 virus [57, 91, 92]. Depletion of RNA m^6A methyltransferases METTL3 or METTL14 using the respective targeting shRNAs decreases viral RNA methylation and suppresses viral transcription and replication. On the contrary, the knockdown of the RNA m^6A demethylase ALKBH5 leads to the increase of the viral replication. [91] Notably, the HIV-1 viral infection itself leads to the enhancement of m^6A modification in the host cell RNA. A major problem in the contemporary HIV-1 virology is the latency of the virus. Therefore, it is highly important to find agents reversing or suppressing the latent virus. [93, 94]

Research carried out during the recent years has demonstrated that RNA m^6A methylation and demethylation modify embryonic brain development, neurogenesis in the mammalian midbrain, neuronal signaling, memory, and disease [1, 95–97]. It has been shown that genes associated with RNA m^6A control may play a role in conferring risk of dementia [98]. Recently, it was demonstrated that the RNA m^6A demethylase FTO has important functions in the dopaminergic midbrain circuitry, which is the vital pathway in Parkinson's disease pathogenesis [95]. Consequently, by modifying the RNA m^6A methylation using m^6A demethylase FTO or ALKBH5 inhibitors, it is also possible to monitor the course of neurodegenerative diseases.

The m^6A modification of RNA has been shown to be strongly related to tumorigenesis [99–105]. It has been shown that the m^6A methyltransferases are mostly upregulated in cancer cells and tissues and act as oncogenes by regulating various signaling pathways in various types of cancers, including acute myeloid leukemia (AML) [5, 106–108], hepatocellular carcinoma [109–111], colorectal cancer [112], gastric cancer [101], lung cancer [113], bladder cancer [114], renal cell carcinoma [115], and melanoma [116]. In contrast, the overexpression of METTL3 or inhibition of the RNA demethylase FTO suppresses

glioblastoma stem cell growth and self-renewal [117]. The other RNA m^6A demethylase, ALKBH5, also promotes glioblastoma stem cells proliferation *in vitro* and tumorigenesis *in vivo* by enhancing the transcription factor Forkhead Box Protein M1 (FOXM1) expression that has been associated with cancer progression and pathogenesis [118]. Both FTO and ALKBH5 have been shown to be oncogenes in the case of breast cancer tissues and cell lines [119]. The RNA m^6A demethylases also enhance AML cell proliferation *in vitro* and promote leukemogenesis *in vivo*. [52, 120] Interestingly, the same overall effect has been observed in the case of the m^6A methyltransferase proteins METTL3 and METTL14 [107, 121].

2. AIM OF THE STUDY

The main aim of this thesis was to find inhibitors and activators for enzymes involved in methylation and demethylation of RNA m^6A using molecular modelling and verify their activity in biological experiments. This work focused on the development and search for new compounds against diseases associated with RNA m^6A regulation.

Paper I. The aim of this paper was to find novel small-molecule ligands for RNA m^6A methyltransferase METTL3/METTL14/WTAP complex using a molecular modelling.

Paper II. The aim of this paper was to find better inhibitors for RNA m^6A demethylase FTO using a molecular modelling and to investigate the effects of these compounds on neurons.

Paper III. The aim of this paper was to find novel inhibitors for RNA m^6A demethylase ALKBH5 using virtual high-throughput screening and to investigate the anti-cancer effects of these compounds on leukemia cells.

Paper IV. The aim of this paper was to investigate the effects of RNA m^6A methyltransferase METTL3/METTL14/WTAP complex activators on the replication of HIV-1 virus.

3. EXPERIMENTAL SECTION

3.1. Molecular docking

Molecular docking is a common method in drug design, in which various low-molecular compounds are matched to the 3D structure of a biological target, usually a protein or nucleic acid. In the case of molecular docking, the energetic effect of ligand-protein binding is studied.

The raw crystal structures of proteins targeted in this work were available from Protein Data Bank (PDB) [122]. Before docking, all crystal structures of proteins were pre-treated using Schrödinger Protein Preparation Wizard [123]. This involved the removal of co-crystallized water, ions and products of the methylation or demethylation reaction from protein 3D structure. Also missing hydrogen atoms were added to the proteins. The geometrical structure of all ligand molecules were optimized using the density functional theory Becke, 3-parameter, Lee–Yang–Parr (B3LYP) method[124] with 6-31G basis set.

In Papers **I** and **II**, the molecular docking was carried out using AutoDock 4.2 software. [125] The numbers of rotatable bonds of the ligand were set as default values within the AutoDock Tools 1.5.6 program [125]. The active site was surrounded with a grid-box sized 65×65×65 (in the case of Paper **I**) or 80×80×80 (in the case of Paper **II**) points with spacing of 0.375 Å. The ligand efficiencies (*LE*) were calculated as follows:

$$LE = -\frac{\Delta G_{dock}}{N} \quad (1)$$

where ΔG_{dock} is the docking free energy calculated using semi-empirical free energy force field [125] for interatomic interactions and N is the number of heavy atoms (non-hydrogen atoms) in the ligand molecule. The higher the *LE* value, the better is the binding between the ligand molecule and the protein. The compounds with the highest docking-free energies and/or ligand efficiencies were selected for the studies on the interactions between ligand compounds and proteins in detail.

3.2. High-throughput virtual screening of compound libraries

High-throughput virtual screening (HTVS) methods play an increasingly more important role in the drug development. HTVS provides processing through millions of compounds to find the most suitable ligands for a particular protein. The screening results help to study the interaction between a compound and biochemical target. It also helps to provide initial ideas for rational drug design.
In the case of HTVS, the preparation of the protein is carried out as described above (Section 3.1). In Paper **III**, a set of compounds from the Functional

molecular IMMunology (FIMM) database was used as ligands. The FIMM compound library (HTB, 2018) [126] contains approximately 144,000 compounds. The geometric 3D structures of the ligands were optimized using the LigPrep procedure from the Schrödinger Suite [127].

The HTVS was carried out using the Glide virtual screening workflow module of the Schrödinger Suite [128, 129] that applies a series of filters to search for the position of the ligand in the active site of the target protein that corresponds to the energy minimum. Glide is a force-field based docking program that uses an optimized interatomic interaction potential (OPLS) [130, 131] for liquid simulations. The Glide HTVS procedure includes three steps: docking with HTVS precision level; docking with standard precision level; docking with an extra precision. All small-molecule ligands were docked flexibly with five docking poses generated for each ligand. Only the best scoring pose was kept for the next step. After each step, the top 30% of ligands with the best docking score were automatically selected for the next step. In this way, a set of compounds for each target was obtained.

The predicted physical interactions between the ligand compounds and protein were further analyzed for compounds with the highest docking-free energies and/or ligand efficiencies.

3.3. Molecular dynamics

Currently, molecular dynamics is routinely used to understand ligand-protein or protein-protein interactions. In Papers **I–III**, the molecular dynamics simulations were used to understand the binding of small molecules to the target proteins in detail.

All molecular dynamics simulations that were done in the Papers **I–III** were carried out using the Desmond simulation package [132] of the Schrödinger Suite [133]. Default parameters were used for all molecular dynamics' simulations. The system total charge was neutralized with sodium or chloride ions before starting the simulations. The simulation lengths were 10 ns or 25 ns and 50 ns with relaxation time 1 ps for all studied protein conformations. The interactions and behavior between the ligands and enzymes were analyzed using the Simulation Interaction Diagram tool implemented in the Desmond molecular dynamics package.

The stability of molecular dynamics simulations was monitored by looking on the root mean square deviation (RMSD) of the ligand and protein atom positions in time. RMSD is used to calculate the average change in movement of a atoms for a particular frame with respect to a reference frame for all frames in the trajectory. The RMSD is calculated as follows:

$$RMSD_x = \sqrt{\frac{1}{N}\sum_{i=1}^{N}\left(r'_i(t_x)\right) - r_i(t_{ref}))^2} \quad (2)$$

where N is the number of atoms, t_{ref} is the reference time, t_x is recording time, r' is the position of the selected atoms in frame x after superimposing on the reference frame.

Figure 2A is an exemplary graph showing the progression of the protein RMSD (blue line) and the red line describes how stable the ligand is at the protein binding center (ligand RMSD).

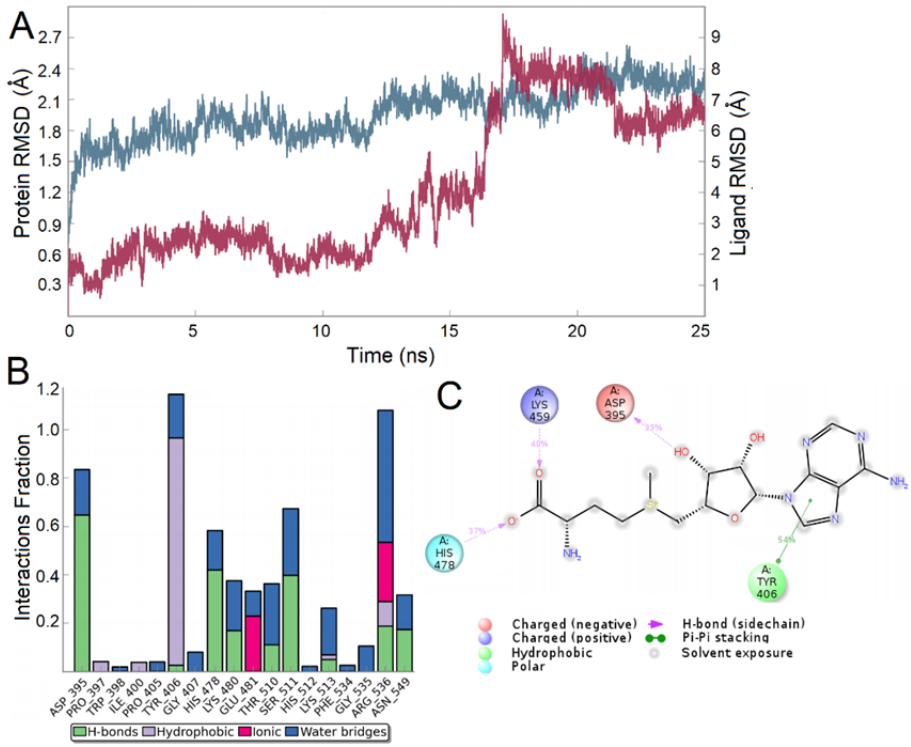

Figure 2. (A) The protein and ligand position root mean square deviation (RMSD) plot against time. (B) Normalized stacked bar chart of interactions and contacts between the protein and ligand over the course of trajectory. (C) A schematic of detailed ligand atom interactions with the protein residues.

The simulation allows visualization of the interactions between the ligand and the protein. It is possible to distinguish four types of interactions between the ligand and protein, i.e. hydrogen bonds, hydrophobic, ionic and water bridges. On Figure 2B, the value of interaction fraction shows how much of the simulation time the given interaction is maintained (1.0 is equal to 100% of the simulation time). If any of the residues bind to the ligand at multiple sites during the simulation, the interaction fraction value may exceed 1.0. An

example in Figure 2C shows in detail which amino acid residue interacts to ligand atom.

3.4. Enzymatic activity assays

In Papers **I**-**III**, the effect of the best binding ligands predicted by computational modeling on the enzymatic activity of m^6A regulating enzymes was measured using the respective assays.

In Paper **I**, the activity of the selected ligands for METTL3/METTL14/ WTAP complex was evaluated using Radioactivity-Based Assay [134]. The change in the m^6A methylation of the substrate RNA by ligand compounds was measured using 2450 MicroBeta® liquid scintillation counter. The scintillation counts were proportional to amount of methylated RNA. The values of the half maximal effective concentration (EC_{50}) were calculated using Graph-Pad Prism 7.0 software.

Regarding Papers **II** and **III**, the enzymatic inhibitory activities of the ligands were measured using commercially available EpiQuik ELISA kit (Epigentek, Farmingdale, NY, USA) employing a m^6A effective antibody. To determine the enzyme activities of the ligands for FTO and ALKBH5 enzymes, an enzymatic reaction was first performed according to the procedure described by Huang et al [34]. Thereafter, the amount of m^6A that was measured using EpiQuik m^6A RNA Methylation Quantification Colorimetric Kit. Absorbance measurements at 450 nm were used to determine enzymatic activity (Epoch™ Microplate Spectrophotometer, BioTek). The IC_{50} values for ligands were calculated using Quest Graph™ IC_{50} Calculator (v.1, AAT Bioquest, Inc., Sunnyvale, CA).

3.5. Binding experiments

The binding of the ligand to the protein was measured in Papers **I**–**III** using different binding assay tools available at research partners.

In Paper **I**, the surface plasmon resonance (SPR) method was used to describe the binding between ligand and protein. SPR enables real-time non-labeled detection of biomolecular interactions. It is an optical method that detects changes in the refractive index caused by mass changes at the receptor surface. [135, 136] All the SPR measurements were performed with a Biacore T100 instrument (GE Healthcare Life Sciences, Chicago, IL, USA).

In Paper **I**, also the binding of compound and protein was carried out using bio-layer interferometry (BLI) method. BLI, like SPR, enables real-time label-free detection of biomolecular interactions [137]. The working principle of BLI is similar to the SPR method. In Paper **I**, Bio-Layer Interferometry instrument Octet K2 with Streptavidin sensors was used (Pall ForteBio LLC, Fremont, CA, USA).

The binding of ligands to the FTO protein (Paper **II**) was determined by the microscale thermophoresis (MST) method. Microscale thermophoresis is based on the detection of a change in the temperature caused by the fluorescence of a target depending on the concentration of non-fluorescent ligand [138]. The MST experiments were performed using Monolith NT.115 instrument (Nano-Temper Technologies GmbH, Munich, Germany).

In Paper **III**, Drug affinity responsive target stability (DARTS) measurements of ligand binding was used. Binding of ligand is expected to stabilize or destabilize target proteins, in a specific conformation or by simply masking protease recognition sites, thereby changing protease sensitivity of the target protein [139]. In Paper **III**, the DARTS experiment was modified from Pai et al. 2016 [140].

3.6. Cell viability measurements

The effect of ligands on cells was also examined in each Paper. The research presented in Paper **I** did not focus so much on the effect of the compounds in cells, but on finding active ligands for the METTL3/METTL14/WTAP enzyme complex. Thus, in this article, only the cytotoxicity of the compounds on HEK-293 cells was tested. For the analysis of cell cycle stages, the HEK-293 cells were treated for 24h with activators of METTL3/METTL14/WTAP complex. The treated cells were collected, washed, and stained with propidium iodide. The number of intact cells was measured using a flow cytometric analysis with the BD Accuri C6 flow cytometer (BD Biosciences, San Jose, CA).

In Paper **II**, the effect of the inhibitors of the m^6A demethylases FTO and ALKBH5 on the dopamine neurons were studied. The cultured neurons were confronted with neuronal suppressor 6-hydroxydopamine (6-OHDA) for 72 hours. The FTO and ALKBH5 inhibitors were thereafter applied on these neurons. After growing 5 days, the neuronal cultures were fixed and stained with anti-tyrosine hydroxylase antibody. Images were acquired by CellInsight high content imaging equipment (ThermoFisher Scientific Inc, Waltham, MA, USA). Immunopositive neurons were counted by CellProfiler software, and the data was analyzed by CellProfiler analyst software [141]. The results are expressed as % of cell survival compared to glial cell line-derived neurotrophic factor (GDNF)-maintained neurons. [142]

In the case of Paper **III**, the effect of the developed ALKBH5 inhibitors on cancer cells was studied for four leukemia cell lines (HL-60, CCRF-CEM, K-562 and Jurkat) and one glioblastoma cell line (A-172). Suspended leukemia cells were grown up to 48 h with added compounds and the cells were counted at the time points 0, 4, 8, 24 and 48 hours. The cell viabilities were measured using Countess Automated Cell Counter (ThermoFisher Scientific Inc). HEK-293T and glioblastoma cells are adherent cells. These cells were seeded on a E-plate. Cells were grown for 48 h with added compounds and cell viability was

measured real-time using the xCELLigence machine (Agilent Technologies Inc, Santa Clara, CA, USA).

3.7. Activation of the HIV-1 virus replication

The effect of the compounds on the HIV-1 replication was studied using a HIV-1 the viral capsid p24 protein-based assay. HIV-1 p24 protein is a component of virus particle capsid. p24 protein is necessary for HIV-1 viral replication and infectivity. HIV-1 p24 protein concentration in host plasma/ host cells supernatant is commonly used as indicator of viral load. The effect of ligands on HIV-1 virus and host cells was also examined in Paper **IV**. The effect of the activators on the gene expression from HIV-1 provirus, creation, and release of HIV-1 virions in cells was measured. The virus host ACH-2 cells were seeded on plate and HIV-1 virion production was stimulated by the addition of phorbol-12-myristate-13-acetate (PMA). The cells were treated with METTL3/ METTL14/WTAP activators and incubated for 48 h. Afterwards, the supernatant containing HIV-1 virions were collected and the amount of HIV-1 p24 protein released into the supernatant was measured using an HIV1 p24 ELISA assay kit (ab218268, Abcam plc, Cambridge, United Kingdom).

In order to find out whether METTL3/METTL14/WTAP enzyme complex activators increase not only the number of virions but also the infectivity, a subsequent infection test was carried out. TZM-bl cells were treated with the supernatant of the incubation media containing equal amount of virus treated with the activators in ACH-2 cells and polybrene. The cells were incubated for 48 h. Subsequently, the supernatant was removed, and the lysis buffer was added. The virus titer was estimated by measuring luciferase activity in cell lysate using the Luciferase Assay System (Promega Corporation, Madison, WI, USA) and Glomax 20/20 Luminometer (Promega Corporation) instruments.

3.8. m^6A level measurements in cells

The effect of the developed active compounds on the level of the m^6A in cells was measured in the case of RNA m^6A methyltransferase METTL3/ METTL14/WTAP activators. The change in the m^6A levels relative to the non-substituted adenosine due to activator compounds was measured in HEK-293 and HIV-1 infected ACH-2 cell RNAs as well as in the HIV-1 RNA.

In Paper **I**, HEK-293 cells were incubated with the METTL3/METTL14/ WTAP activators for 2 hours and the total RNA was extracted using the TRIzol reagent (ThermoFisher Scientific Inc) according to the manufacturer's protocol. In the studies described in Paper **IV**, ACH-2 cells were treated with METTL3/ METTL14/WTAP protein complex activator and HIV-1 virion production was induced by the addition of PMA. After 48h, the media containing HIV-1 virions as well as the treated ACH-2 cells were collected. The viral RNA was allocated

using the TRIzol reagent and cells mRNA was obtained using the Dynabeads® mRNA DIRECT Micro Kit (ThermoFisher Scientific Inc). Total RNA, viral RNA and cellular mRNAs was digested enzymatically according to the Liu et al [143].

The abundance of m^6A relative to the adenosine in Paper **I** was measured with Nexera X2 UHPLC instrument with triple quadrupole (MS/MS) system 8050 (Shimadzu Corporation, Kyoto, Japan). In Paper **IV**, the Agilent 1290 UHPLC (Agilent Technologies Inc) and Agilent 6460 Triple Quadrupole MS (Agilent Technologies Inc) was used.

4. RESULTS AND DISCUSSION

In this section, we present and discuss the results of both the computational modelling and experimental studies. In Table 1, the chemical structures and the docking results for all compounds studied in this Thesis are presented.

Table 1. Summary table of docking results and structures of the ligands

Comp.	Structure	ΔG (kcal/ mol)	DE	Paper	Comp. in Paper
1I	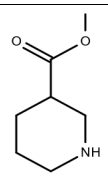	-6.94	0.69	**I/IV**	**1**
2I	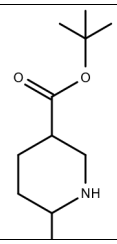	-6.97	0.50	**I/IV**	**2**
3I	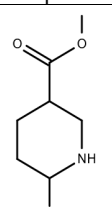	-6.27	0.57	**I/IV**	**3**
4I	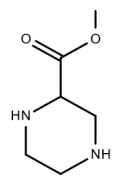	-5.34	0.53	**I/IV**	**4**
1II	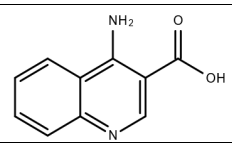	-7.37	0.53	**II**	**1**
2II	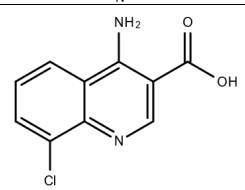	-7.70	0.51	**II**	**2**

Comp.	Structure	ΔG (kcal/ mol)	DE	Paper	Comp. in Paper
3II	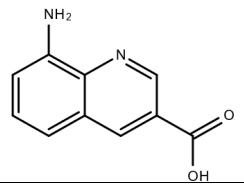	-7.03	0.50	**II**	**3**
4II	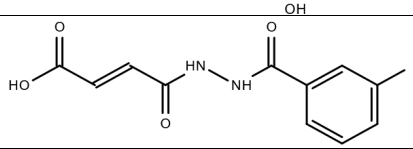	-8.78	0.49	**II**	**4**
5II	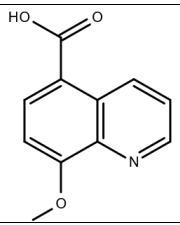	-7.17	0.48	**II**	**5**
6II	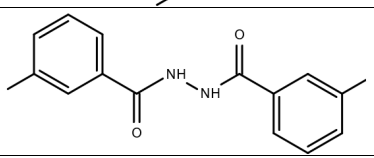	-9.45	0.47	**II**	**6**
1III	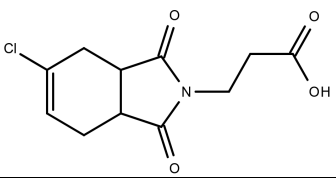	-8.70	0.51	**III**	**1**
2III	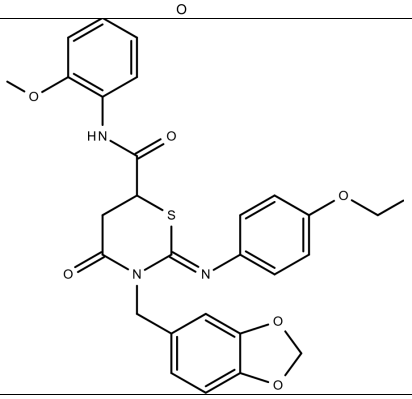	-8.13	0.21	**III**	**2**
3III	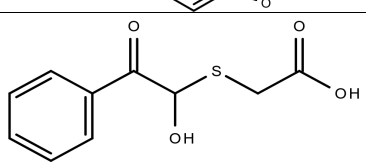	-6.53	0.44	**III**	**3**

Comp.	Structure	ΔG (kcal/ mol)	DE	Paper	Comp. in Paper
4III	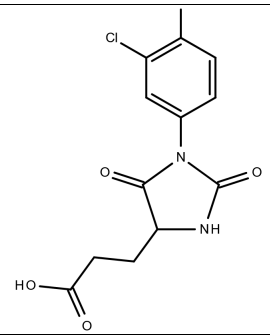	-7.83	0.39	**III**	**4**
5III	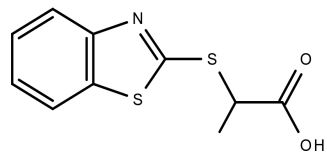	-7.08	0.47	**III**	**5**
6III	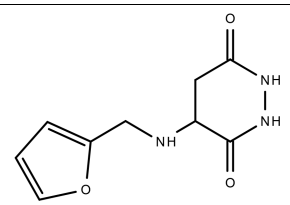	-4.78	0.32	**III**	**6**
5IV	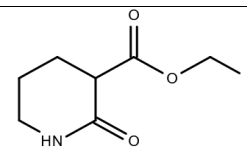	-5.44	0.45	**IV**	**5**

4.1. METTL3/METTL14/WTAP activators

The main aim of Paper **I** was to develop active ligands for RNA m^6A methyltransferase METTL3/METTL14/WTAP complex by using rational molecular design.

Based on METTL3/METTL14 protein complex 3D crystal structure (pdb: 5K7W) [27] we proceeded with the search for effectively binding small molecular fragments. A virtual screening on ZINC [144] and DrugBank 4.0 [145] databases was carried out based on the configuration of the METTL3 residues that are hydrogen bonded to the tail part of the methylating agent SAM. Some of these amino acid residues (Lys513, Asp395 and Ile378) possess side groups potentially available for strong ligand binding. The docking results showed that the compounds with the piperidine or piperazine rings interacted with amino acid residues deeply embedded into the structure of METTL3/ METTL14 protein. The docking free energies and docking efficiencies of the best ligands for METTL3/METTL14 protein complex are given in Table 1.

To further evaluate the docking calculation results, the molecular dynamics simulations were carried out with the compounds **1I** and **4I**. These compounds were selected because they belong to different chemical scaffolds (piperidine and piperazine derivatives, respectively).

The results of molecular dynamics simulations showed that both compounds are bound to the same tight specific pocket at the SAM binding site. Similar to the docking results, the compound **1I** provided more interactions with METTL3/METTL14 protein complex than compound **4I** (Figure 3).

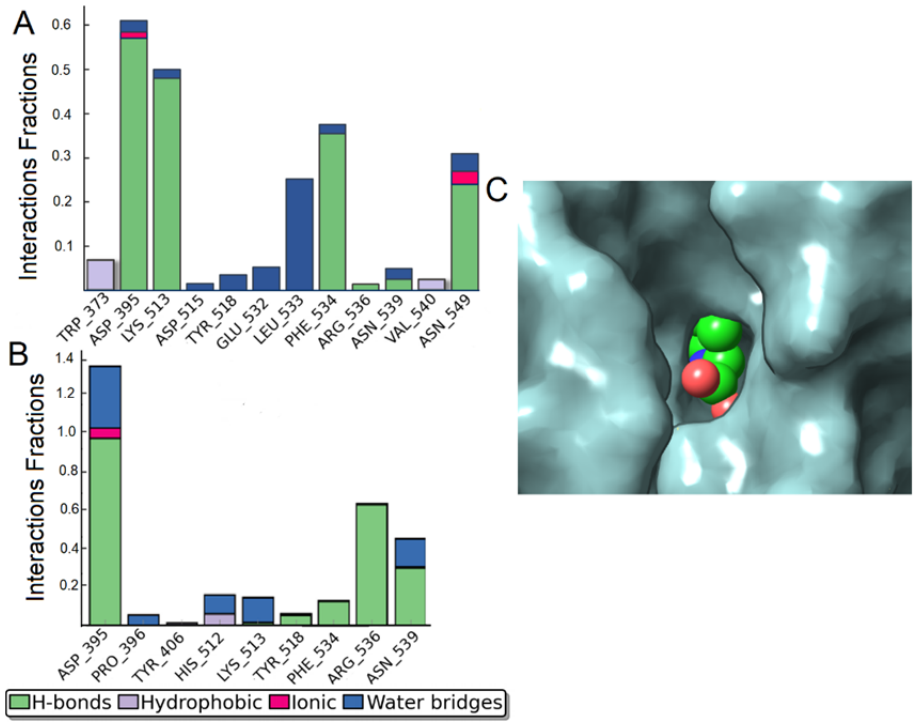

Figure 3. (A) Interaction diagram between the compound **1I** and METTL3/METTL14 complex. (B) Interaction diagram between the compound **4I** and METTL3/METTL14 complex. (C) The position of the compound **4I** the structure of METTL3 protein.

The binding between the predicted ligand compounds and RNA m^6A methyltransferase METTL3/METTL14/WTAP complex was studied using the SPR measurements with a Biacore T100 instrument. The results showed that all four compounds were bound to the METTL3/METTL14/WTAP complex. The dissociation constants of compounds were as follows: K_D = 0.93 μM for compound **1I**, K_D = 16.3 μM for compound **2I**, K_D = 0.05 nM for compound **3I** and K_D = 1.97 μM for compound **4I.** The dissociation constant for SAM was

1.92 μM. Compounds **1I** and **4I** were selected to test the effect of these compounds on SAM binding to the METTL3/METTL14/WTAP complex. It turned out that both compounds significantly increase SAM binding to the protein complex. The SAM dissociation constants in the presence of small compounds were respectively K_D = 4.70 nM and K_D = 13.7 nM for compound **3I** and compound **4I**, respectively.

The METTL3 proteins with point mutations were used to localize the compounds position at the active site of the protein. The binding of compound **4I** to the METTL3 protein was thus studied using BLI technology with streptavidin sensors, the results consistent with those obtained with SPR method. The binding of compound **4I** to the mutated proteins was not detectable within the sensitivity of the BLI instrument. Consequently, the compounds bind specifically to the active site of the METTL3 protein.

The effect of the METTL3/METTL14/WTAP enzyme complex activators on the RNA m^6A methylation was measured using Radioactivity-Based Assay. All four compounds were not acting as METTL3/METTL14/WTAP complex inhibitors, surprisingly all these compounds significantly increase enzyme complex activity. The effective concentration values of compounds were EC_{50} = 0.11 nM for compound **1I**, EC_{50} = 3.16 μM for compound **2I**, EC_{50} = 117.0 nM for compound **3I** and EC_{50} = 12.5 nM for compound **4I**.

No cytotoxic effects on the HEK-293 cells were observed up to 100 μM concentrations for all four activators. To extend the results of an *in vitro* enzymatic assay to the cellular level, a quantification of m^6A levels in total RNA after treatment with activators and without compound was carried out. Activators **1I**, **2I** and **3I** increased the m^6A amount relative to adenosine while activator **4I** did not significantly affect the level of m^6A in the total RNA sample.

The m^6A modifications in the viral and host cell RNAs play very important role in HIV-1 virus genome transcription and virus replication. Therefore, the aim of Paper **IV** was to study the effect of the discovered RNA m^6A methyltransferase METTL3/METTL14/WTAP enzyme complex activators on the replication HIV-1 virus.

The effect of the compounds on the HIV-1 replication was studied using the measurement of the HIV-1 p24 protein level that is proportional to the number of HIV-1 virions. The amount of HIV-1 p24 protein that was released into the supernatant from virus containing ACH-2 cells was measured using HIV-1 p24 ELISA Kit. In the case of compounds **3I**, **4I** and **5IV**, a significant concentration-dependent effect on virion production was observed (Figure 4).

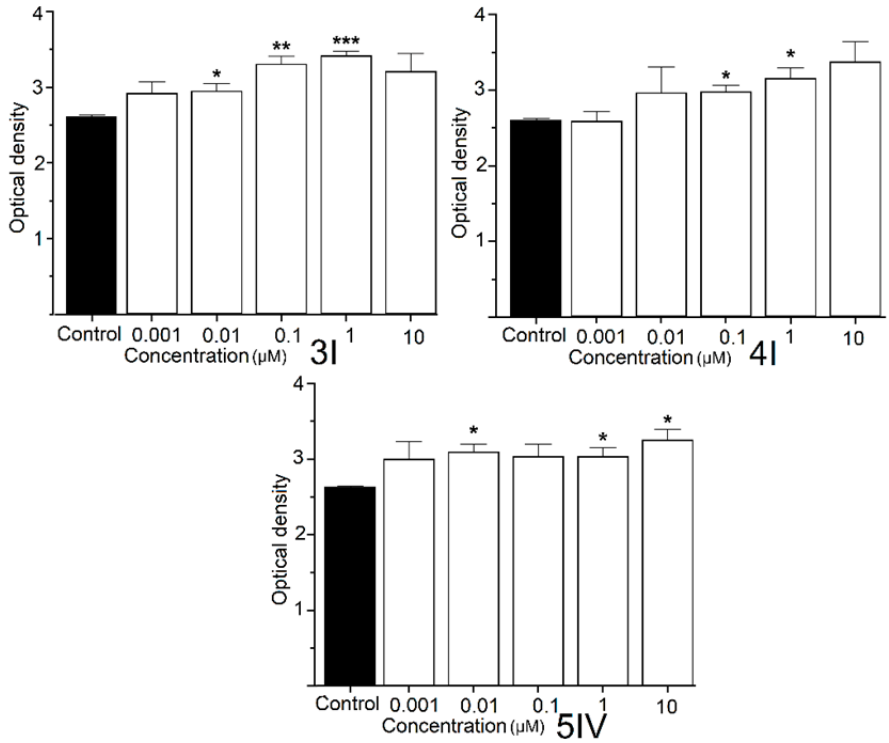

Figure 4. Dependence of the amount HIV-1 p24 released to the growth medium after treatment of ACH-2 cells with the METTL3/METTL14/WTAP activators **3I**, **4I** and **5IV** at different concentrations. The results are shown as means ± standard deviation from three independent experiments (n =3); *p < 0.05, ** p < 0.01, ***p < 0.005.

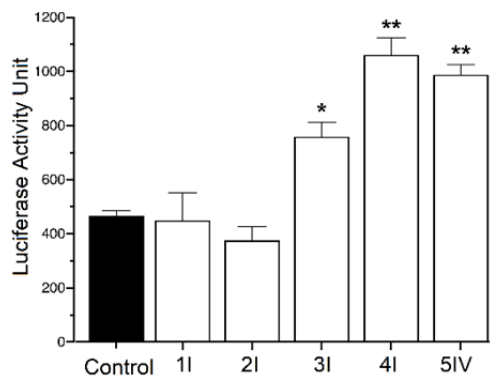

Figure 5. Increase of production of HIV-1 virions in TZM-bl cells infected with media collected from virus containing ACH-2 cells treated with METTL3/METTL14/WTAP activator compounds. The results are shown as means ± standard deviation from three independent experiments: *p < 0.05, ** p < 0.01 (n=3).

In addition, the effect of METTL3/METTL14/WTAP enzyme complex activators on the level of the m^6A methylation in the viral RNA and in cellular mRNA was studied. ACH-2 cells containing HIV-1 provirus were treated with the METTL3/METTL14/WTAP activator **4I**. As a result, activator **4I** increased the mRNA m^6A level in ACH-2 cells more than twice. In addition, a 18 % increase of the m^6A methylation of the virus RNA genome itself was also noticed. This was the first demonstration that a small-molecule ligand can change the m^6A methylation level of a viral RNA.

4.2. FTO inhibitors

The main objective of Paper **II** was to find new inhibitors for RNA m^6A demethylase FTO using rational molecular design and study the effect of these compounds on dopamine neurons.

The crystal structure of the FTO protein (pdb:4IE4) [32] was chosen for the molecular modelling by removing the native ligands from the 3D crystal structure. A virtual screening on ZINC compound database[144] was carried out using the best known FTO inhibitors as templates [32, 146, 147].

The enzyme inhibition measurements were carried out for six compounds that showed strong protein binding in molecular docking calculations (Table 1). A significant concentration-dependent inhibitory effect was observed for quinolone derivatives **2II** and **3II**. The inhibitory concentration values were measured as IC_{50} = 1.46 μM for compound **2II** and IC_{50} = 28.9 μM for compound **3II**, respectively. No inhibitory effect was registered for other compounds.

The 10 ns length molecular dynamics simulations were carried out for two compounds (compound **2II** and **3II**), the compounds with the best enzymatic inhibition activity in m^6A RNA enzymatic assay. The most important interactions with the protein suggested for compound **2II** are given in Figure 6A. Those involve hydrogen bonds between the ligand and residues Arg96, Glu234, Arg322 and Asp233 of FTO protein and hydrophobic interactions between compound and FTO protein. The results of the molecular dynamics simulations of compound **3II** are summarized in Figure 6B. The results suggest the presence of hydrogen bonds between the carbonyl group of compound **3II** and Glu234 and Asp233 of the FTO protein. In addition, formation of a water bridge with Arg96 and salt bridge with Arg322 was predicted. The simulation interactions diagram reveals a very stable hydrogen bonding and several ionic bridges and water bridges between the compound **3II** and FTO protein.

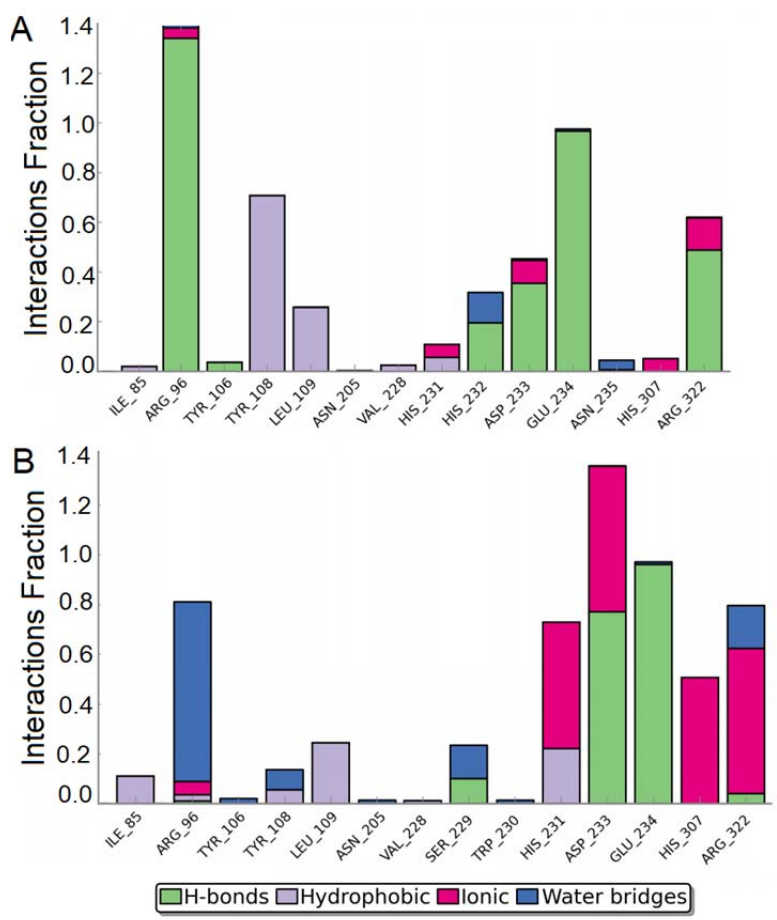

Figure 6. (A) Interaction diagram between the compound **2II** and FTO protein. (B) Interaction diagram between the compound **3II** and FTO protein.

The binding of the compounds to the FTO protein was studied using the MST method. The results showed that both compounds are binding at sub-micromolar concentrations. The protein binding dissociation constant values are K_D = 185 ± 77 nM (**2II**) and K_D = 337 ± 184 nM (**3II**).

The m^6A RNA modifications and their dynamics in the cell has been recently related to neurogenesis and neuronal survival. Therefore, it was interesting to assess the effects of the inhibitors of the FTO protein on the survival of dopamine neurons. The experiments using the *in vitro* model of Parkinson's disease were carried out at the University of Helsinki for two RNA m^6A demethylase FTO inhibitors developed in this study.

The neuroprotective ability of FTO inhibitors at different concentrations was studied on cultured dopamine neurons treated with toxins. The treatment with

toxin 6-OHDA caused neurons cell death by 50-70 % in 5 days. Both FTO inhibitors **2II** and **3II** dose-dependently protected embryonic midbrain dopamine neurons, similarly to the positive control (neurotrophic factor GDNF). A neuroprotective effect can be seen already at 10 nM concentration of the FTO inhibitors (Figure 7).

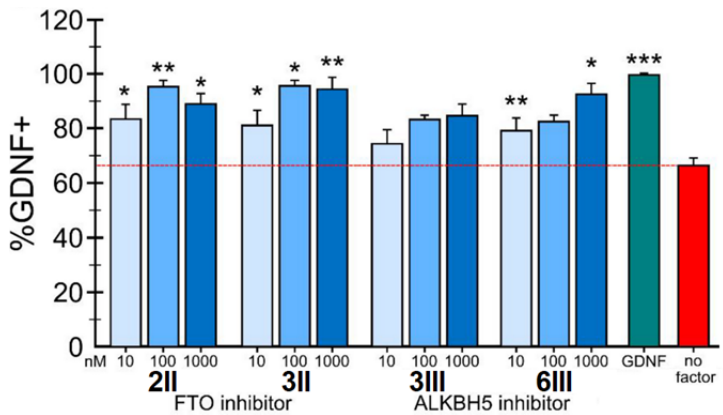

Figure 7. Effect of the FTO inhibitors **2II** and **3II** and ALKBH5 inhibitors **3III** and **6III** on the survival of the dopamine neurons. The results are shown as means ± standard deviation from three independent experiments. * $p < 0.05$, ** $p < 0.01$, *** $p < 0.001$, one-way ANOVA with Dunnett's posthoc test.

Hence, it was the first time demonstrated that the inhibition of the m^6A demethylase FTO promotes on the survival of dopamine neurons and rescues them in the growth factor deprivation induced apoptosis *in vitro* model of Parkinson's disease without any signs of toxicity of the tested compounds. This opens a whole new avenue in the development of neuroprotective and neuroregenerative medical drugs.

4.3. ALKBH5 inhibitors

The aim of Paper **III** was to develop novel inhibitors for RNA m^6A demethylase ALKBH5 by using high-throughput virtual screening. The ALKBH5 enzyme has been shown to be oncogenic in several cancer types, including leukemia. Because of that, the effect of the inhibitors of ALKBH5 enzyme on leukemia cells was investigated also in Paper **III**.

The 3D crystal structure of the ALKBH5 protein (pdb:4O61) [148] was chosen for the molecular modelling by removing the native ligands from the 3D crystal structure. A virtual screening on the FIMM compound library (HTB, 2018) was carried out using the full collection of 144,000 compounds.

The enzyme inhibition measurements were carried out for six compounds that showed the best binding efficiencies in molecular docking calculations (Table 1). A concentration-dependent inhibitory effect was observed for compounds **3III** and **6III**. The inhibitory concentration values were IC_{50} = 0.84 μM for compound **3III** and IC_{50} = 1.79 μM for compound **6III**. For the other four compounds the inhibitory effect was missing.

For these two compounds the 10 ns length molecular dynamics simulations were carried out. The results indicated the presence of a quite strong hydrogen bond with His204 residue of the ALKBH5 protein for both compounds. In addition, the compounds had similar number of hydrophobic interactions and water bridges between the molecule and ALKBH5 protein (Figure 8).

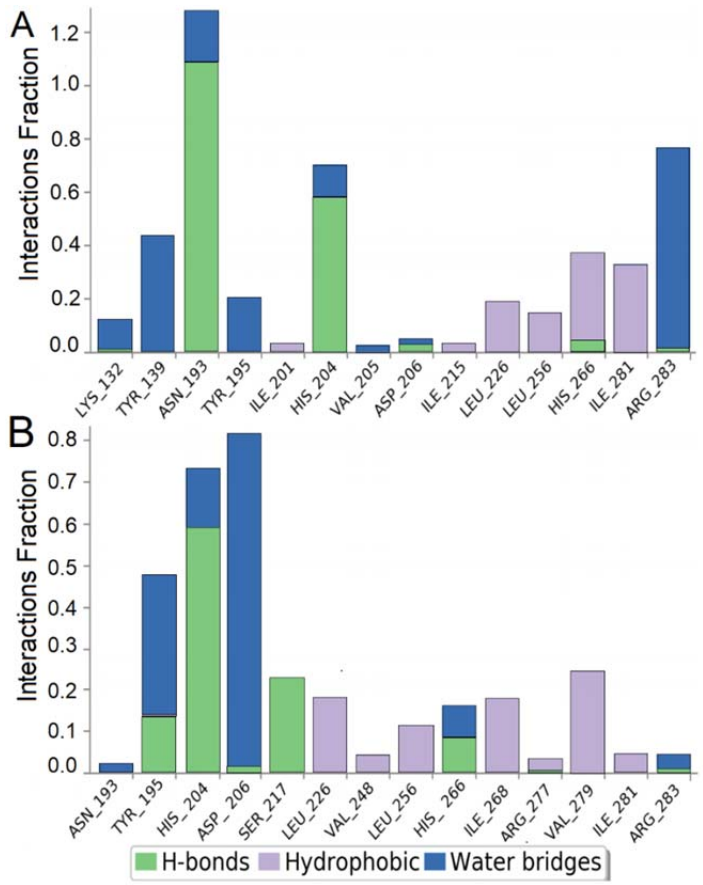

Figure 8. The results of the molecular dynamics simulations. (A) Interaction diagram between the compound **3III** and ALKBH5 protein. (B) Interaction diagram between the compound **6III** and ALKBH5 protein.

The binding of the compounds **3III** and **6III** to the ALKBH5 protein was measured by the DARTS method. The results showed that compound **3III** significantly affects the stability of the ALKBH5 protein and consequently binds to the protein. For compound **6III**, this effect is much smaller.

The compounds **3III** and **6III** were further used to study the effects of RNA m^6A demethylase ALKBH5 inhibition on cell viability on cultures of several cancer cell lines. Four leukemia cell lines (HL-60, CCRF-CEM, K-562 and Jurkat) and one glioblastoma cell line (A-172) were chosen for this purpose. The human embryonic kidney HEK-293 cell line was used as a control. In the case of both ALKBH5 inhibitors, the viability of the HL-60, CCRF-CEM and K-562 leukemia cells was decreased by up to 60% already at low micromolar concentrations (Figure 9). A much smaller effect was registered in the case of Jurkat cells and some small effect at high micromolar concentrations was registered on A-172 and HEK-293T cells. Thus, these results indicate that the effect of the ALKBH5 inhibition on the viability of cancer cells may depend on the cancer type (subtype).

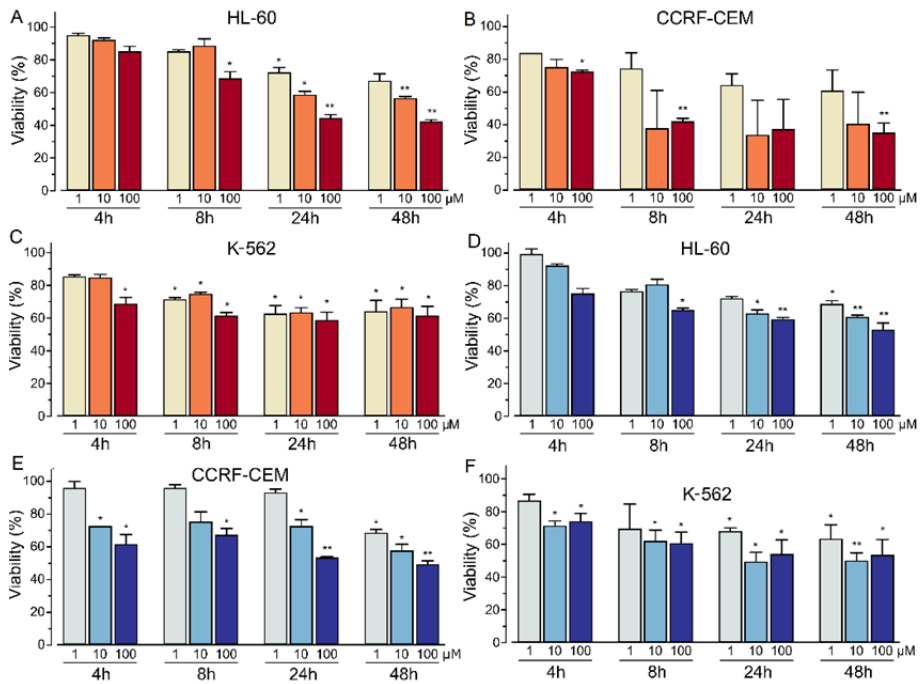

Figure 9. Time dependence of cell viability at different concentrations of the ALKBH5 inhibitors **3III** and **6III**. (A) **3III** effect on HL-60 cells; (B) **3III** effect on CCRF-CEM cells; (C) **3III** effect on K-562 cell; (D) **6III** effect on HL-60 cells; (E) **6III** effect on CCRF-CEM cells; (F) **6III** effect on K-562 cells. Data presented as means ± standard deviation *$p < 0.05$, **$p < 0.01$, ***$p < 0.001$, two-way analysis of variance (ANOVA) test.

In Paper **II**, the two inhibitors of RNA m^6A demethylase ALKBH5 **3III** and **6III** were tested in the dopamine neurons. Notably, a similar yet smaller supportive effect on the survival of dopamine neurons was observed in the case of RNA m^6A demethylase ALKBH5 inhibitors compared to FTO inhibitors (Figure 7).

SUMMARY

The main objective of the present thesis was to develop a primary set of ligands that would inhibit or activate various proteins involved in RNA m^6A methylation and demethylation. The first potentially active compounds were identified using complex molecular modelling methods (molecular docking, molecular dynamics and HTVS). The behavior of the compounds obtained as a result of molecular modelling was monitored by several experimental methods. In addition, the effect of the most active compounds was studied using *in vitro* models of various pathologies.

The first part of this thesis describes the discovery of small-molecule activators for the RNA m^6A methyltransferase METTL3/METTL14/WTAP complex. The compounds with the highest potential binding affinity to this complex were designed by using molecular docking and molecular dynamics simulations. The binding of these compounds to METTL3 protein was thereafter measured experimentally by SPR method, showing the K_D values in low nanomolar range for compounds **1I** and **4I**. The EC_{50} values obtained from the enzymatic assay experiments for these compounds, related to the activation of the METTL3/METTL14/WTAP complex, were EC_{50} = 0.11 nM for compound **1I**, EC_{50} = 3.16 μM for compound **2I**, EC_{50} = 117.0 nM for compound **3I** and EC_{50} = 12.5 nM for compound **4I**. In addition, these compounds were shown to increase m^6A methylation in cellular RNA. The effect of RNA m^6A methyltransferase activators on HIV-1 replication was also examined. All activators increased viral replication and viral infectivity, most notably the compounds **3I** and **4I**. The influence of the compound **4I** on the methylation of RNA was studied using LC/MC measurements. The treatment with this compound caused an increase in the amount of sixth position methylated adenosines in both viral RNA and cellular mRNA.

The second part of the thesis focuses on optimizing the structures of known RNA m^6A demethylase FTO inhibitors by using molecular docking, virtual screening and molecular dynamics simulations. Six potential inhibitors were identified, two of these compounds showed activity in the enzymatic experiments and binding measurements at micromolar level. The inhibitory concentration values were IC_{50} = 1.46 μM for compound **2II** and IC_{50} = 28.9 μM for compound **3II**. The effect of these inhibitors was studied in the *in vitro* Parkinson's disease model, based on the growth factor deprivation induced apoptosis. A strong neuroprotective effect was seen already at low nanomolar concentrations of both studied FTO inhibitors.

The third part of the thesis is devoted to finding inhibitors for another RNA m^6A demethylase, the ALKBH5 enzyme. The HTVS was used to find potential inhibitors. Molecular dynamics simulations were additionally carried out in order to better understand the interactions between small-molecule ligands and the ALKBH5 protein. The enzymatic assay measurements gave the inhibitory concentration values for the most active compounds as IC_{50} = 0.84 μM for

compound **3III** and IC_{50} = 1.79 μM for compound **6III**. As the irregularities in the ALKBH5 enzyme expression have been closely associated with cancer, the effect of the developed ALKBH5 inhibitors on cancer cells were studied. In the case of both ALKBH5 inhibitors, the viability of the HL-60, CCRF-CEM and K-562 leukemia cells was decreased by up to 60% already at low micromolar inhibitor concentrations.

In conclusion, three protein targets related to RNA m^6A methylation and demethylation were studied in the present thesis. New active ligands on the nanomolar or low micromolar scale were found for each three targets. As a result of further optimization, these compounds may become attractive drug candidates against diseases associated with RNA m^6A regulation.

REFERENCES

[1] Jiang, X.; Liu, B.; Nie, Z.; Duan, L.; Xiong, Q.; Jin, Z.; Yang, C.; Chen, Y. The Role of M6A Modification in the Biological Functions and Diseases. *Signal Transduct. Target. Ther.*, **2021**, *6* (1), 1–16. https://doi.org/10.1038/s41392-020-00450-x.

[2] Boccaletto, P.; Machnicka, M. A.; Purta, E.; Piatkowski, P.; Baginski, B.; Wirecki, T. K.; de Crécy-Lagard, V.; Ross, R.; Limbach, P. A.; Kotter, A.; et al. MODOMICS: A Database of RNA Modification Pathways. 2017 Update. *Nucleic Acids Res.*, **2018**, *46* (D1), D303–D307. https://doi.org/10.1093/nar/gkx1030.

[3] Liu, N.; Pan, T. N6-Methyladenosine–Encoded Epitranscriptomics. *Nat. Struct. Mol. Biol.*, **2016**, *23* (2), 98–102. https://doi.org/10.1038/nsmb.3162.

[4] Yang, Y.; Hsu, P. J.; Chen, Y.-S.; Yang, Y.-G. Dynamic Transcriptomic M6A Decoration: Writers, Erasers, Readers and Functions in RNA Metabolism. *Cell Res.*, **2018**, *28* (6), 616–624. https://doi.org/10.1038/s41422-018-0040-8.

[5] Zhao, B. S.; Roundtree, I. A.; He, C. Post-Transcriptional Gene Regulation by MRNA Modifications. *Nat. Rev. Mol. Cell Biol.*, **2017**, *18* (1), 31–42. https://doi.org/10.1038/nrm.2016.132.

[6] Park, C. H.; Hong, K. Epitranscriptome: M6A and Its Function in Stem Cell Biology. *Genes Genomics*, **2017**, *39* (4), 371–378. https://doi.org/10.1007/s13258-016-0507-2.

[7] Fang, X.; Li, M.; Yu, T.; Liu, G.; Wang, J. Reversible N6-Methyladenosine of RNA: The Regulatory Mechanisms on Gene Expression and Implications in Physiology and Pathology. *Genes Dis.*, **2020**, *7* (4), 585–597. https://doi.org/10.1016/j.gendis.2020.06.011.

[8] Fu, Y.; Dominissini, D.; Rechavi, G.; He, C. Gene Expression Regulation Mediated through Reversible m 6 A RNA Methylation. *Nat. Rev. Genet.*, **2014**, *15* (5), 293–306. https://doi.org/10.1038/nrg3724.

[9] Wu, B.; Li, L.; Huang, Y.; Ma, J.; Min, J. Readers, Writers and Erasers of N6-Methylated Adenosine Modification. *Curr. Opin. Struct. Biol.*, **2017**, *47*, 67–76. https://doi.org/10.1016/j.sbi.2017.05.011.

[10] Bokar, J. A.; Shambaugh, M. E.; Polayes, D.; Matera, A. G.; Rottman, F. M. Purification and CDNA Cloning of the AdoMet-Binding Subunit of the Human MRNA (N6-Adenosine)-Methyltransferase. *RNA N. Y. N*, **1997**, *3* (11), 1233–1247.

[11] Liu, J.; Yue, Y.; Han, D.; Wang, X.; Fu, Y.; Zhang, L.; Jia, G.; Yu, M.; Lu, Z.; Deng, X.; et al. A METTL3–METTL14 Complex Mediates Mammalian Nuclear RNA N 6 -Adenosine Methylation. *Nat. Chem. Biol.*, **2014**, *10* (2), 93–95. https://doi.org/10.1038/nchembio.1432.

[12] Agarwala, S. D.; Blitzblau, H. G.; Hochwagen, A.; Fink, G. R. RNA Methylation by the MIS Complex Regulates a Cell Fate Decision in Yeast. *PLoS Genet.*, **2012**, *8* (6), e1002732. https://doi.org/10.1371/journal.pgen.1002732.

[13] Schwartz, S.; Mumbach, M. R.; Jovanovic, M.; Wang, T.; Maciag, K.; Bushkin, G. G.; Mertins, P.; Ter-Ovanesyan, D.; Habib, N.; Cacchiarelli, D.; et al. Perturbation of M6A Writers Reveals Two Distinct Classes of MRNA Methylation at Internal and 5' Sites. *Cell Rep.*, **2014**, *8* (1), 284–296. https://doi.org/10.1016/j.celrep.2014.05.048.

[14] Patil, D. P.; Chen, C.-K.; Pickering, B. F.; Chow, A.; Jackson, C.; Guttman, M.; Jaffrey, S. R. M 6 A RNA Methylation Promotes XIST -Mediated Transcriptional Repression. *Nature*, **2016**, *537* (7620), 369–373. https://doi.org/10.1038/nature19342.

[15] Wen, J.; Lv, R.; Ma, H.; Shen, H.; He, C.; Wang, J.; Jiao, F.; Liu, H.; Yang, P.; Tan, L.; et al. Zc3h13 Regulates Nuclear RNA M6A Methylation and Mouse Embryonic Stem Cell Self-Renewal. *Mol. Cell*, **2018**, *69* (6), 1028-1038.e6. https://doi.org/10.1016/j.molcel.2018.02.015.
[16] Pendleton, K. E.; Chen, B.; Liu, K.; Hunter, O. V.; Xie, Y.; Tu, B. P.; Conrad, N. K. The U6 SnRNA M6A Methyltransferase METTL16 Regulates SAM Synthetase Intron Retention. *Cell*, **2017**, *169* (5), 824-835.e14. https://doi.org/10.1016/j.cell.2017.05.003.
[17] Wang, X.; Feng, J.; Xue, Y.; Guan, Z.; Zhang, D.; Liu, Z.; Gong, Z.; Wang, Q.; Huang, J.; Tang, C.; et al. Structural Basis of N 6 -Adenosine Methylation by the METTL3–METTL14 Complex. *Nature*, **2016**, *534* (7608), 575–578. https://doi.org/10.1038/nature18298.
[18] Yankova, E.; Blackaby, W.; Albertella, M.; Rak, J.; De Braekeleer, E.; Tsagkogeorga, G.; Pilka, E. S.; Aspris, D.; Leggate, D.; Hendrick, A. G.; et al. Small-Molecule Inhibition of METTL3 as a Strategy against Myeloid Leukaemia. *Nature*, **2021**, 1–5. https://doi.org/10.1038/s41586-021-03536-w.
[19] Bedi, R. K.; Huang, D.; Eberle, S. A.; Wiedmer, L.; Śledź, P.; Caflisch, A. Small-Molecule Inhibitors of METTL3, the Major Human Epitranscriptomic Writer. *ChemMedChem*, **2020**, *15* (9), 744–748. https://doi.org/10.1002/cmdc.202000011.
[20] Śledź, P.; Jinek, M. Structural Insights into the Molecular Mechanism of the M6A Writer Complex. *eLife*, **2016**, *5*, e18434. https://doi.org/10.7554/eLife.18434.
[21] Aoyama, T.; Yamashita, S.; Tomita, K. Mechanistic Insights into M6A Modification of U6 SnRNA by Human METTL16. *Nucleic Acids Res.*, **2020**, *48* (9), 5157–5168. https://doi.org/10.1093/nar/gkaa227.
[22] Doxtader, K. A.; Wang, P.; Scarborough, A. M.; Seo, D.; Conrad, N. K.; Nam, Y. Structural Basis for Regulation of METTL16, an S-Adenosylmethionine Homeostasis Factor. *Mol. Cell*, **2018**, *71* (6), 1001-1011.e4. https://doi.org/10.1016/j.molcel.2018.07.025.
[23] Ruszkowska, A.; Ruszkowski, M.; Dauter, Z.; Brown, J. A. Structural Insights into the RNA Methyltransferase Domain of METTL16. *Sci. Rep.*, **2018**, *8* (1), 1–13. https://doi.org/10.1038/s41598-018-23608-8.
[24] Mendel, M.; Chen, K.-M.; Homolka, D.; Gos, P.; Pandey, R. R.; McCarthy, A. A.; Pillai, R. S. Methylation of Structured RNA by the M6A Writer METTL16 Is Essential for Mouse Embryonic Development. *Mol. Cell*, **2018**, *71* (6), 986-1000.e11. https://doi.org/10.1016/j.molcel.2018.08.004.
[25] Karthiya, R.; Khandelia, P. M6A RNA Methylation: Ramifications for Gene Expression and Human Health. *Mol. Biotechnol.*, **2020**, *62*. https://doi.org/10.1007/s12033-020-00269-5.
[26] Niu, Y.; Zhao, X.; Wu, Y.-S.; Li, M.-M.; Wang, X.-J.; Yang, Y.-G. N6-Methyl-Adenosine (M6A) in RNA: An Old Modification with a Novel Epigenetic Function. *Genomics Proteomics Bioinformatics*, **2013**, *11* (1), 8–17. https://doi.org/10.1016/j.gpb.2012.12.002.
[27] Wang, P.; Doxtader, K. A.; Nam, Y. Structural Basis for Cooperative Function of Mettl3 and Mettl14 Methyltransferases. *Mol. Cell*, **2016**, *63* (2), 306–317. https://doi.org/10.1016/j.molcel.2016.05.041.
[28] Ping, X.-L.; Sun, B.-F.; Wang, L.; Xiao, W.; Yang, X.; Wang, W.-J.; Adhikari, S.; Shi, Y.; Lv, Y.; Chen, Y.-S.; et al. Mammalian WTAP Is a Regulatory Subunit of the RNA N6-Methyladenosine Methyltransferase. *Cell Res.*, **2014**, *24* (2), 177–189. https://doi.org/10.1038/cr.2014.3.

[29] Shima, H.; Matsumoto, M.; Ishigami, Y.; Ebina, M.; Muto, A.; Sato, Y.; Kumagai, S.; Ochiai, K.; Suzuki, T.; Igarashi, K. S-Adenosylmethionine Synthesis Is Regulated by Selective N6-Adenosine Methylation and MRNA Degradation Involving METTL16 and YTHDC1. *Cell Rep.*, **2017**, *21* (12), 3354–3363. https://doi.org/10.1016/j.celrep.2017.11.092.
[30] Warda, A. S.; Kretschmer, J.; Hackert, P.; Lenz, C.; Urlaub, H.; Höbartner, C.; Sloan, K. E.; Bohnsack, M. T. Human METTL16 Is a N6-Methyladenosine (M6A) Methyltransferase That Targets Pre-MRNAs and Various Non-Coding RNAs. *EMBO Rep.*, **2017**, *18* (11), 2004–2014. https://doi.org/10.15252/embr.201744940.
[31] Zheng, G.; Dahl, J. A.; Niu, Y.; Fedorcsak, P.; Huang, C.-M.; Li, C. J.; Vågbø, C. B.; Shi, Y.; Wang, W.-L.; Song, S.-H.; et al. ALKBH5 Is a Mammalian RNA Demethylase That Impacts RNA Metabolism and Mouse Fertility. *Mol. Cell*, **2013**, *49* (1), 18–29. https://doi.org/10.1016/j.molcel.2012.10.015.
[32] Aik, W.; Demetriades, M.; Hamdan, M. K. K.; Bagg, Eleanor. A. L.; Yeoh, K. K.; Lejeune, C.; Zhang, Z.; McDonough, M. A.; Schofield, C. J. Structural Basis for Inhibition of the Fat Mass and Obesity Associated Protein (FTO). *J. Med. Chem.*, **2013**, *56* (9), 3680–3688. https://doi.org/10.1021/jm400193d.
[33] Toh, J. D. W.; Sun, L.; Lau, L. Z. M.; Tan, J.; Low, J. J. A.; Tang, C. W. Q.; Cheong, E. J. Y.; Tan, M. J. H.; Chen, Y.; Hong, W.; et al. A Strategy Based on Nucleotide Specificity Leads to a Subfamily-Selective and Cell-Active Inhibitor of N6-Methyladenosine Demethylase FTO. *Chem. Sci.*, **2014**, *6* (1), 112–122. https://doi.org/10.1039/C4SC02554G.
[34] Huang, Y.; Yan, J.; Li, Q.; Li, J.; Gong, S.; Zhou, H.; Gan, J.; Jiang, H.; Jia, G.-F.; Luo, C.; et al. Meclofenamic Acid Selectively Inhibits FTO Demethylation of M6A over ALKBH5. *Nucleic Acids Res.*, **2015**, *43* (1), 373–384. https://doi.org/10.1093/nar/gku1276.
[35] Zhang, X.; Wei, L.-H.; Wang, Y.; Xiao, Y.; Liu, J.; Zhang, W.; Yan, N.; Amu, G.; Tang, X.; Zhang, L.; et al. Structural Insights into FTO's Catalytic Mechanism for the Demethylation of Multiple RNA Substrates. *Proc. Natl. Acad. Sci.*, **2019**, *116* (8), 2919–2924. https://doi.org/10.1073/pnas.1820574116.
[36] Han, Z.; Niu, T.; Chang, J.; Lei, X.; Zhao, M.; Wang, Q.; Cheng, W.; Wang, J.; Feng, Y.; Chai, J. Crystal Structure of the FTO Protein Reveals Basis for Its Substrate Specificity. *Nature*, **2010**, *464* (7292), 1205–1209. https://doi.org/10.1038/nature08921.
[37] Peng, S.; Xiao, W.; Ju, D.; Sun, B.; Hou, N.; Liu, Q.; Wang, Y.; Zhao, H.; Gao, C.; Zhang, S.; et al. Identification of Entacapone as a Chemical Inhibitor of FTO Mediating Metabolic Regulation through FOXO1. *Sci. Transl. Med.*, **2019**, *11* (488). https://doi.org/10.1126/scitranslmed.aau7116.
[38] Wang, T.; Hong, T.; Huang, Y.; Su, H.; Wu, F.; Chen, Y.; Wei, L.; Huang, W.; Hua, X.; Xia, Y.; et al. Fluorescein Derivatives as Bifunctional Molecules for the Simultaneous Inhibiting and Labeling of FTO Protein. *J. Am. Chem. Soc.*, **2015**, *137* (43), 13736–13739. https://doi.org/10.1021/jacs.5b06690.
[39] Feng, C.; Liu, Y.; Wang, G.; Deng, Z.; Zhang, Q.; Wu, W.; Tong, Y.; Cheng, C.; Chen, Z. Crystal Structures of the Human RNA Demethylase Alkbh5 Reveal Basis for Substrate Recognition*. *J. Biol. Chem.*, **2014**, *289* (17), 11571–11583. https://doi.org/10.1074/jbc.M113.546168.
[40] Xu, C.; Liu, K.; Tempel, W.; Demetriades, M.; Aik, W.; Schofield, C. J.; Min, J. Structures of Human ALKBH5 Demethylase Reveal a Unique Binding Mode for

Specific Single-Stranded N6-Methyladenosine RNA Demethylation. *J. Biol. Chem.*, **2014**, *289* (25), 17299–17311. https://doi.org/10.1074/jbc.M114.550350.

[41] Aik, W.; Scotti, J. S.; Choi, H.; Gong, L.; Demetriades, M.; Schofield, C. J.; McDonough, M. A. Structure of Human RNA N^6-Methyladenine Demethylase ALKBH5 Provides Insights into Its Mechanisms of Nucleic Acid Recognition and Demethylation. *Nucleic Acids Res.*, **2014**, *42* (7), 4741–4754. https://doi.org/10.1093/nar/gku085.

[42] Wang, T.; Kong, S.; Tao, M.; Ju, S. The Potential Role of RNA N6-Methyladenosine in Cancer Progression. *Mol. Cancer*, **2020**, *19* (1), 88. https://doi.org/10.1186/s12943-020-01204-7.

[43] Ferenc, K.; Pilžys, T.; Garbicz, D.; Marcinkowski, M.; Skorobogatov, O.; Dylewska, M.; Gajewski, Z.; Grzesiuk, E.; Zabielski, R. Intracellular and Tissue Specific Expression of FTO Protein in Pig: Changes with Age, Energy Intake and Metabolic Status. *Sci. Rep.*, **2020**, *10* (1), 13029. https://doi.org/10.1038/s41598-020-69856-5.

[44] Roundtree, I. A.; Evans, M. E.; Pan, T.; He, C. Dynamic RNA Modifications in Gene Expression Regulation. *Cell*, **2017**, *169* (7), 1187–1200. https://doi.org/10.1016/j.cell.2017.05.045.

[45] Merkestein, M.; McTaggart, J. S.; Lee, S.; Kramer, H. B.; McMurray, F.; Lafond, M.; Boutens, L.; Cox, R.; Ashcroft, F. M. Changes in Gene Expression Associated with FTO Overexpression in Mice. *PLoS ONE*, **2014**, *9* (5), e97162. https://doi.org/10.1371/journal.pone.0097162.

[46] Zou, S.; Toh, J. D. W.; Wong, K. H. Q.; Gao, Y.-G.; Hong, W.; Woon, E. C. Y. N6-Methyladenosine: A Conformational Marker That Regulates the Substrate Specificity of Human Demethylases FTO and ALKBH5. *Sci. Rep.*, **2016**, *6* (1), 25677. https://doi.org/10.1038/srep25677.

[47] Relier, S.; Ripoll, J.; Guillorit, H.; Amalric, A.; Achour, C.; Boissière, F.; Vialaret, J.; Attina, A.; Debart, F.; Choquet, A.; et al. FTO-Mediated Cytoplasmic m 6 A m Demethylation Adjusts Stem-like Properties in Colorectal Cancer Cell. *Nat. Commun.*, **2021**, *12* (1), 1716. https://doi.org/10.1038/s41467-021-21758-4.

[48] Wei, J.; Liu, F.; Lu, Z.; Fei, Q.; Ai, Y.; He, P. C.; Shi, H.; Cui, X.; Su, R.; Klungland, A.; et al. Differential M6A, M6Am, and M1A Demethylation Mediated by FTO in the Cell Nucleus and Cytoplasm. *Mol. Cell*, **2018**, *71* (6), 973-985.e5. https://doi.org/10.1016/j.molcel.2018.08.011.

[49] Chen, B.; Ye, F.; Yu, L.; Jia, G.; Huang, X.; Zhang, X.; Peng, S.; Chen, K.; Wang, M.; Gong, S.; et al. Development of Cell-Active N6-Methyladenosine RNA Demethylase FTO Inhibitor. *J. Am. Chem. Soc.*, **2012**, *134* (43), 17963–17971. https://doi.org/10.1021/ja3064149.

[50] Zheng, G.; Cox, T.; Tribbey, L.; Wang, G. Z.; Iacoban, P.; Booher, M. E.; Gabriel, G. J.; Zhou, L.; Bae, N.; Rowles, J.; et al. Synthesis of a FTO Inhibitor with Anticonvulsant Activity. *ACS Chem. Neurosci.*, **2014**, *5* (8), 658–665. https://doi.org/10.1021/cn500042t.

[51] Wang, X.; Zhao, B. S.; Roundtree, I. A.; Lu, Z.; Han, D.; Ma, H.; Weng, X.; Chen, K.; Shi, H.; He, C. N6-Methyladenosine Modulates Messenger RNA Translation Efficiency. *Cell*, **2015**, *161* (6), 1388–1399. https://doi.org/10.1016/j.cell.2015.05.014.

[52] Huang, Y.; Su, R.; Sheng, Y.; Dong, L.; Dong, Z.; Xu, H.; Ni, T.; Zhang, Z. S.; Zhang, T.; Li, C.; et al. Small-Molecule Targeting of Oncogenic FTO Demethylase

in Acute Myeloid Leukemia. *Cancer Cell*, **2019**, *35* (4), 677-691.e10. https://doi.org/10.1016/j.ccell.2019.03.006.
[53] Su, R.; Dong, L.; Li, Y.; Gao, M.; Han, L.; Wunderlich, M.; Deng, X.; Li, H.; Huang, Y.; Gao, L.; et al. Targeting FTO Suppresses Cancer Stem Cell Maintenance and Immune Evasion. *Cancer Cell*, **2020**, *38* (1), 79-96.e11. https://doi.org/10.1016/j.ccell.2020.04.017.
[54] Malacrida, A.; Rivara, M.; Di Domizio, A.; Cislaghi, G.; Miloso, M.; Zuliani, V.; Nicolini, G. 3D Proteome-Wide Scale Screening and Activity Evaluation of a New ALKBH5 Inhibitor in U87 Glioblastoma Cell Line. *Bioorg. Med. Chem.*, **2020**, *28* (4), 115300. https://doi.org/10.1016/j.bmc.2019.115300.
[55] Patil, D. P.; Pickering, B. F.; Jaffrey, S. R. Reading M6A in the Transcriptome: M6A-Binding Proteins. *Trends Cell Biol.*, **2018**, *28* (2), 113–127. https://doi.org/10.1016/j.tcb.2017.10.001.
[56] Dai, X.-Y.; Shi, L.; Li, Z.; Yang, H.-Y.; Wei, J.-F.; Ding, Q. Main N6-Methyladenosine Readers: YTH Family Proteins in Cancers. *Front. Oncol.*, **2021**, *11*. https://doi.org/10.3389/fonc.2021.635329.
[57] Kennedy, E.; Bogerd, H.; Kornepati, A. V. R.; Kang, D.; Ghoshal, D.; Marshall, J.; Poling, B.; Tsai, K.; Gokhale, N.; Horner, S.; et al. Posttranscriptional m(6)A Editing of HIV-1 MRNAs Enhances Viral Gene Expression. *Cell Host Microbe*, **2016**, *19*. https://doi.org/10.1016/j.chom.2016.04.002.
[58] Balacco, D. L.; Soller, M. The m(6)A Writer: Rise of a Machine for Growing Tasks. *Biochemistry*, **2019**, *58* (5), 363–378. https://doi.org/10.1021/acs.biochem.8b01166.
[59] Huang, H.; Weng, H.; Sun, W.; Qin, X.; Shi, H.; Wu, H.; Zhao, B. S.; Mesquita, A.; Liu, C.; Yuan, C. L.; et al. Recognition of RNA N 6 -Methyladenosine by IGF2BP Proteins Enhances MRNA Stability and Translation. *Nat. Cell Biol.*, **2018**, *20* (3), 285–295. https://doi.org/10.1038/s41556-018-0045-z.
[60] Alarcón, C. R.; Goodarzi, H.; Lee, H.; Liu, X.; Tavazoie, S.; Tavazoie, S. F. HNRNPA2B1 Is a Mediator of M6A-Dependent Nuclear RNA Processing Events. *Cell*, **2015**, *162* (6), 1299–1308. https://doi.org/10.1016/j.cell.2015.08.011.
[61] Xu, C.; Liu, K.; Ahmed, H.; Loppnau, P.; Schapira, M.; Min, J. Structural Basis for the Discriminative Recognition of N6-Methyladenosine RNA by the Human YT521-B Homology Domain Family of Proteins*. *J. Biol. Chem.*, **2015**, *290* (41), 24902–24913. https://doi.org/10.1074/jbc.M115.680389.
[62] Woodcock, C. B.; Horton, J. R.; Zhou, J.; Bedford, M. T.; Blumenthal, R. M.; Zhang, X.; Cheng, X. Biochemical and Structural Basis for YTH Domain of Human YTHDC1 Binding to Methylated Adenine in DNA. *Nucleic Acids Res.*, **2020**, *48* (18), 10329–10341. https://doi.org/10.1093/nar/gkaa604.
[63] Li, Y.; Bedi, R. K.; Moroz-Omori, E. V.; Caflisch, A. Structural and Dynamic Insights into Redundant Function of YTHDF Proteins. *J. Chem. Inf. Model.*, **2020**, *60* (12), 5932–5935. https://doi.org/10.1021/acs.jcim.0c01029.
[64] Li, F.; Zhao, D.; Wu, J.; Shi, Y. Structure of the YTH Domain of Human YTHDF2 in Complex with an m 6 A Mononucleotide Reveals an Aromatic Cage for m 6 A Recognition. *Cell Res.*, **2014**, *24* (12), 1490–1492. https://doi.org/10.1038/cr.2014.153.
[65] Zhu, T.; Roundtree, I. A.; Wang, P.; Wang, X.; Wang, L.; Sun, C.; Tian, Y.; Li, J.; He, C.; Xu, Y. Crystal Structure of the YTH Domain of YTHDF2 Reveals Mechanism for Recognition of N6-Methyladenosine. *Cell Res.*, **2014**, *24* (12), 1493–1496. https://doi.org/10.1038/cr.2014.152.

[66] Li, Y.; Bedi, R. K.; Wiedmer, L.; Sun, X.; Huang, D.; Caflisch, A. Atomistic and Thermodynamic Analysis of N6-Methyladenosine (M6A) Recognition by the Reader Domain of YTHDC1. *J. Chem. Theory Comput.*, **2021**, *17* (2), 1240–1249. https://doi.org/10.1021/acs.jctc.0c01136.

[67] Li, Y.; Bedi, R. K.; Wiedmer, L.; Huang, D.; Śledź, P.; Caflisch, A. Flexible Binding of M6A Reader Protein YTHDC1 to Its Preferred RNA Motif. *J. Chem. Theory Comput.*, **2019**, *15* (12), 7004–7014. https://doi.org/10.1021/acs.jctc.9b00987.

[68] Ma, C.; Liao, S.; Zhu, Z. Crystal Structure of Human YTHDC2 YTH Domain. *Biochem. Biophys. Res. Commun.*, **2019**, *518* (4), 678–684. https://doi.org/10.1016/j.bbrc.2019.08.107.

[69] Theler, D.; Dominguez, C.; Blatter, M.; Boudet, J.; Allain, F. H.-T. Solution Structure of the YTH Domain in Complex with N6-Methyladenosine RNA: A Reader of Methylated RNA. *Nucleic Acids Res.*, **2014**, *42* (22), 13911–13919. https://doi.org/10.1093/nar/gku1116.

[70] Dagil, R.; Ball, N. J.; Ogrodowicz, R. W.; Hobor, F.; Purkiss, A. G.; Kelly, G.; Martin, S. R.; Taylor, I. A.; Ramos, A. IMP1 KH1 and KH2 Domains Create a Structural Platform with Unique RNA Recognition and Re-Modelling Properties. *Nucleic Acids Res.*, **2019**, *47* (8), 4334–4348. https://doi.org/10.1093/nar/gkz136.

[71] Chao, J. A.; Patskovsky, Y.; Patel, V.; Levy, M.; Almo, S. C.; Singer, R. H. ZBP1 Recognition of β-Actin Zipcode Induces RNA Looping. *Genes Dev.*, **2010**, *24* (2), 148–158. https://doi.org/10.1101/gad.1862910.

[72] Biswas, J.; Patel, V. L.; Bhaskar, V.; Chao, J. A.; Singer, R. H.; Eliscovich, C. The Structural Basis for RNA Selectivity by the IMP Family of RNA-Binding Proteins. *Nat. Commun.*, **2019**, *10* (1), 4440. https://doi.org/10.1038/s41467-019-12193-7.

[73] Jia, M.; Gut, H.; Chao, J. A. Structural Basis of IMP3 RRM12 Recognition of RNA. *RNA*, **2018**, *24* (12), 1659–1666. https://doi.org/10.1261/rna.065649.118.

[74] Schneider, T.; Hung, L.-H.; Aziz, M.; Wilmen, A.; Thaum, S.; Wagner, J.; Janowski, R.; Müller, S.; Schreiner, S.; Friedhoff, P.; et al. Combinatorial Recognition of Clustered RNA Elements by the Multidomain RNA-Binding Protein IMP3. *Nat. Commun.*, **2019**, *10* (1), 2266. https://doi.org/10.1038/s41467-019-09769-8.

[75] Wu, B.; Su, S.; Patil, D. P.; Liu, H.; Gan, J.; Jaffrey, S. R.; Ma, J. Molecular Basis for the Specific and Multivariant Recognitions of RNA Substrates by Human HnRNP A2/B1. *Nat. Commun.*, **2018**, *9* (1), 420. https://doi.org/10.1038/s41467-017-02770-z.

[76] Lu, J.; Cao, Q.; Hughes, M. P.; Sawaya, M. R.; Boyer, D. R.; Cascio, D.; Eisenberg, D. S. CryoEM Structure of the Low-Complexity Domain of HnRNPA2 and Its Conversion to Pathogenic Amyloid. *Nat. Commun.*, **2020**, *11* (1), 4090. https://doi.org/10.1038/s41467-020-17905-y.

[77] Yoon, K.-J.; Ringeling, F. R.; Vissers, C.; Jacob, F.; Pokrass, M.; Jimenez-Cyrus, D.; Su, Y.; Kim, N.-S.; Zhu, Y.; Zheng, L.; et al. Temporal Control of Mammalian Cortical Neurogenesis by M6A Methylation. *Cell*, **2017**, *171* (4), 877-889.e17. https://doi.org/10.1016/j.cell.2017.09.003.

[78] Guo, M.; Liu, X.; Zheng, X.; Huang, Y.; Chen, X. M6A RNA Modification Determines Cell Fate by Regulating MRNA Degradation. *Cell. Reprogramming*, **2017**, *19* (4), 225–231. https://doi.org/10.1089/cell.2016.0041.

[79] Wu, R.; Jiang, D.; Wang, Y.; Wang, X. N (6)-Methyladenosine (m(6)A) Methylation in MRNA with A Dynamic and Reversible Epigenetic Modification. *Mol. Biotechnol.*, **2016**, *58* (7), 450–459. https://doi.org/10.1007/s12033-016-9947-9.

[80] Chen, T.; Hao, Y.-J.; Zhang, Y.; Li, M.-M.; Wang, M.; Han, W.; Wu, Y.; Lv, Y.; Hao, J.; Wang, L.; et al. M6A RNA Methylation Is Regulated by MicroRNAs and Promotes Reprogramming to Pluripotency. *Cell Stem Cell*, **2015**, *16* (3), 289–301. https://doi.org/10.1016/j.stem.2015.01.016.

[81] Batista, P. J.; Molinie, B.; Wang, J.; Qu, K.; Zhang, J.; Li, L.; Bouley, D. M.; Lujan, E.; Haddad, B.; Daneshvar, K.; et al. M6A RNA Modification Controls Cell Fate Transition in Mammalian Embryonic Stem Cells. *Cell Stem Cell*, **2014**, *15* (6), 707–719. https://doi.org/10.1016/j.stem.2014.09.019.

[82] Gokhale, N. S.; Horner, S. M. RNA Modifications Go Viral. *PLOS Pathog.*, **2017**, *13* (3), e1006188. https://doi.org/10.1371/journal.ppat.1006188.

[83] Hesser, C. R.; Karijolich, J.; Dominissini, D.; He, C.; Glaunsinger, B. A. N6-Methyladenosine Modification and the YTHDF2 Reader Protein Play Cell Type Specific Roles in Lytic Viral Gene Expression during Kaposi's Sarcoma-Associated Herpesvirus Infection. *PLOS Pathog.*, **2018**, *14* (4), e1006995. https://doi.org/10.1371/journal.ppat.1006995.

[84] Imam, H.; Khan, M.; Gokhale, N. S.; McIntyre, A. B. R.; Kim, G.-W.; Jang, J. Y.; Kim, S.-J.; Mason, C. E.; Horner, S. M.; Siddiqui, A. N6-Methyladenosine Modification of Hepatitis B Virus RNA Differentially Regulates the Viral Life Cycle. *Proc. Natl. Acad. Sci.*, **2018**, *115* (35), 8829–8834. https://doi.org/10.1073/pnas.1808319115.

[85] Williams, G. D.; Gokhale, N. S.; Horner, S. M. Regulation of Viral Infection by the RNA Modification N6-Methyladenosine. *Annu. Rev. Virol.*, **2019**, *6* (1), 235–253. https://doi.org/10.1146/annurev-virology-092818-015559.

[86] Fleming, A. M.; Nguyen, N. L. B.; Burrows, C. J. Colocalization of M6A and G-Quadruplex-Forming Sequences in Viral RNA (HIV, Zika, Hepatitis B, and SV40) Suggests Topological Control of Adenosine N6-Methylation. *ACS Cent. Sci.*, **2019**, *5* (2), 218–228. https://doi.org/10.1021/acscentsci.8b00963.

[87] Manners, O.; Baquero-Perez, B.; Whitehouse, A. M6A: Widespread Regulatory Control in Virus Replication. *Biochim. Biophys. Acta BBA - Gene Regul. Mech.*, **2019**, *1862* (3), 370–381. https://doi.org/10.1016/j.bbagrm.2018.10.015.

[88] Xue, M.; Zhao, B. S.; Zhang, Z.; Lu, M.; Harder, O.; Chen, P.; Lu, Z.; Li, A.; Ma, Y.; Xu, Y.; et al. Viral N 6 -Methyladenosine Upregulates Replication and Pathogenesis of Human Respiratory Syncytial Virus. *Nat. Commun.*, **2019**, *10* (1), 1–18. https://doi.org/10.1038/s41467-019-12504-y.

[89] Bayoumi, M.; Rohaim, M. A.; Munir, M. Structural and Virus Regulatory Insights Into Avian N6-Methyladenosine (M6A) Machinery. *Front. Cell Dev. Biol.*, **2020**, *8*. https://doi.org/10.3389/fcell.2020.00543.

[90] Kim, G.-W.; Imam, H.; Khan, M.; Siddiqui, A. N6-Methyladenosine Modification of Hepatitis B and C Viral RNAs Attenuates Host Innate Immunity via RIG-I Signaling. *J. Biol. Chem.*, **2020**, *295* (37), 13123–13133. https://doi.org/10.1074/jbc.RA120.014260.

[91] Lichinchi, G.; Gao, S.; Saletore, Y.; Gonzalez, G. M.; Bansal, V.; Wang, Y.; Mason, C. E.; Rana, T. M. Dynamics of the Human and Viral m 6 A RNA Methylomes during HIV-1 Infection of T Cells. *Nat. Microbiol.*, **2016**, *1* (4), 1–9. https://doi.org/10.1038/nmicrobiol.2016.11.

[92] Lu, W.; Tirumuru, N.; St. Gelais, C.; Koneru, P. C.; Liu, C.; Kvaratskhelia, M.; He, C.; Wu, L. N6-Methyladenosine–Binding Proteins Suppress HIV-1 Infectivity and Viral Production. *J. Biol. Chem.*, **2018**, *293* (34), 12992–13005. https://doi.org/10.1074/jbc.RA118.004215.

[93] Ait-Ammar, A.; Kula, A.; Darcis, G.; Verdikt, R.; De Wit, S.; Gautier, V.; Mallon, P. W. G.; Marcello, A.; Rohr, O.; Van Lint, C. Current Status of Latency Reversing Agents Facing the Heterogeneity of HIV-1 Cellular and Tissue Reservoirs. *Front. Microbiol.*, **2020**, *10*. https://doi.org/10.3389/fmicb.2019.03060.

[94] Kula-Pacurar, A.; Rodari, A.; Darcis, G.; Van Lint, C. Shocking HIV-1 with Immunomodulatory Latency Reversing Agents. *Semin. Immunol.*, **2021**, 101478. https://doi.org/10.1016/j.smim.2021.101478.

[95] Hess, M. E.; Hess, S.; Meyer, K. D.; Verhagen, L. A. W.; Koch, L.; Brönneke, H. S.; Dietrich, M. O.; Jordan, S. D.; Saletore, Y.; Elemento, O.; et al. The Fat Mass and Obesity Associated Gene (Fto) Regulates Activity of the Dopaminergic Midbrain Circuitry. *Nat. Neurosci.*, **2013**, *16* (8), 1042–1048. https://doi.org/10.1038/nn.3449.

[96] Lence, T.; Akhtar, J.; Bayer, M.; Schmid, K.; Spindler, L.; Ho, C. H.; Kreim, N.; Andrade-Navarro, M. A.; Poeck, B.; Helm, M.; et al. M6A Modulates Neuronal Functions and Sex Determination in Drosophila. *Nature*, **2016**, *540* (7632), 242–247. https://doi.org/10.1038/nature20568.

[97] Li, L.; Zang, L.; Zhang, F.; Chen, J.; Shen, H.; Shu, L.; Liang, F.; Feng, C.; Chen, D.; Tao, H.; et al. Fat Mass and Obesity-Associated (FTO) Protein Regulates Adult Neurogenesis. *Hum. Mol. Genet.*, **2017**, *26* (13), 2398–2411. https://doi.org/10.1093/hmg/ddx128.

[98] Du, T.; Rao, S.; Wu, L.; Ye, N.; Liu, Z.; Hu, H.; Xiu, J.; Shen, Y.; Xu, Q. An Association Study of the M6A Genes with Major Depressive Disorder in Chinese Han Population. *J. Affect. Disord.*, **2015**, *183*, 279–286. https://doi.org/10.1016/j.jad.2015.05.025.

[99] Pan, Y.; Ma, P.; Liu, Y.; Li, W.; Shu, Y. Multiple Functions of M6A RNA Methylation in Cancer. *J. Hematol. Oncol.J Hematol Oncol*, **2018**, *11* (1), 48. https://doi.org/10.1186/s13045-018-0590-8.

[100] Yu, S.; Li, X.; Liu, S.; Yang, R.; Liu, X.; Wu, S. N6-Methyladenosine: A Novel RNA Imprint in Human Cancer. *Front. Oncol.*, **2019**, *9*. https://doi.org/10.3389/fonc.2019.01407.

[101] Liu, T.; Yang, S.; Sui, J.; Xu, S.-Y.; Cheng, Y.-P.; Shen, B.; Zhang, Y.; Zhang, X.-M.; Yin, L.-H.; Pu, Y.-P.; et al. Dysregulated N6-Methyladenosine Methylation Writer METTL3 Contributes to the Proliferation and Migration of Gastric Cancer. *J. Cell. Physiol.*, **2020**, *235* (1), 548–562. https://doi.org/10.1002/jcp.28994.

[102] Liu, L.; Wang, Y.; Wu, J.; Liu, J.; Qin, Z.; Fan, H. N6-Methyladenosine: A Potential Breakthrough for Human Cancer. *Mol. Ther. - Nucleic Acids*, **2020**, *19*, 804–813. https://doi.org/10.1016/j.omtn.2019.12.013.

[103] Liu, S.; Li, Q.; Chen, K.; Zhang, Q.; Li, G.; Zhuo, L.; Zhai, B.; Sui, X.; Hu, X.; Xie, T. The Emerging Molecular Mechanism of M6A Modulators in Tumorigenesis and Cancer Progression. *Biomed. Pharmacother. Biomedecine Pharmacother.*, **2020**, *127*, 110098. https://doi.org/10.1016/j.biopha.2020.110098.

[104] Zeng, C.; Huang, W.; Li, Y.; Weng, H. Roles of METTL3 in Cancer: Mechanisms and Therapeutic Targeting. *J. Hematol. Oncol.J Hematol Oncol*, **2020**, *13*. https://doi.org/10.1186/s13045-020-00951-w.

[105] Zhou, Z.; Lv, J.; Yu, H.; Han, J.; Yang, X.; Feng, D.; Wu, Q.; Yuan, B.; Lu, Q.; Yang, H. Mechanism of RNA Modification N6-Methyladenosine in Human Cancer. *Mol. Cancer*, **2020**, *19* (1), 104. https://doi.org/10.1186/s12943-020-01216-3.

[106] Bansal, H.; Yihua, Q.; Iyer, S. P.; Ganapathy, S.; Proia, D. A.; Proia, D.; Penalva, L. O.; Uren, P. J.; Suresh, U.; Carew, J. S.; et al. WTAP Is a Novel Oncogenic Protein in Acute Myeloid Leukemia. *Leukemia*, **2014**, *28* (5), 1171–1174. https://doi.org/10.1038/leu.2014.16.

[107] Barbieri, I.; Tzelepis, K.; Pandolfini, L.; Shi, J.; Millán-Zambrano, G.; Robson, S. C.; Aspris, D.; Migliori, V.; Bannister, A. J.; Han, N.; et al. Promoter-Bound METTL3 Maintains Myeloid Leukaemia by m 6 A-Dependent Translation Control. *Nature*, **2017**, *552* (7683), 126–131. https://doi.org/10.1038/nature24678.

[108] Choe, J.; Lin, S.; Zhang, W.; Liu, Q.; Wang, L.; Ramirez-Moya, J.; Du, P.; Kim, W.; Tang, S.; Sliz, P.; et al. MRNA Circularization by METTL3–EIF3h Enhances Translation and Promotes Oncogenesis. *Nature*, **2018**, *561* (7724), 556–560. https://doi.org/10.1038/s41586-018-0538-8.

[109] Ma, J.-Z.; Yang, F.; Zhou, C.-C.; Liu, F.; Yuan, J.-H.; Wang, F.; Wang, T.-T.; Xu, Q.-G.; Zhou, W.-P.; Sun, S.-H. METTL14 Suppresses the Metastatic Potential of Hepatocellular Carcinoma by Modulating N6 -Methyladenosine-Dependent Primary MicroRNA Processing. *Hepatol. Baltim. Md*, **2017**, *65* (2), 529–543. https://doi.org/10.1002/hep.28885.

[110] Chen, M.; Wei, L.; Law, C.-T.; Tsang, F. H.-C.; Shen, J.; Cheng, C. L.-H.; Tsang, L.-H.; Ho, D. W.-H.; Chiu, D. K.-C.; Lee, J. M.-F.; et al. RNA N6-Methyladenosine Methyltransferase-like 3 Promotes Liver Cancer Progression through YTHDF2-Dependent Posttranscriptional Silencing of SOCS2. *Hepatol. Baltim. Md*, **2018**, *67* (6), 2254–2270. https://doi.org/10.1002/hep.29683.

[111] Cheng, X.; Li, M.; Rao, X.; Zhang, W.; Li, X.; Wang, L.; Huang, G. KIAA1429 Regulates the Migration and Invasion of Hepatocellular Carcinoma by Altering M6A Modification of ID2 MRNA. *OncoTargets Ther.*, **2019**, *12*, 3421–3428. https://doi.org/10.2147/OTT.S180954.

[112] Li, B.-Q.; Liang, Z.-Y.; Seery, S.; Liu, Q.-F.; You, L.; Zhang, T.-P.; Guo, J.-C.; Zhao, Y.-P. WT1 Associated Protein Promotes Metastasis and Chemo-Resistance to Gemcitabine by Stabilizing Fak MRNA in Pancreatic Cancer. *Cancer Lett.*, **2019**, *451*, 48–57. https://doi.org/10.1016/j.canlet.2019.02.043.

[113] Wei, W.; Huo, B.; Shi, X. MiR-600 Inhibits Lung Cancer via Downregulating the Expression of METTL3. *Cancer Manag. Res.*, **2019**, *11*, 1177–1187. https://doi.org/10.2147/CMAR.S181058.

[114] Han, J.; Wang, J.-Z.; Yang, X.; Yu, H.; Zhou, R.; Lu, H.-C.; Yuan, W.-B.; Lu, J.-C.; Zhou, Z.-J.; Lu, Q.; et al. METTL3 Promote Tumor Proliferation of Bladder Cancer by Accelerating Pri-MiR221/222 Maturation in M6A-Dependent Manner. *Mol. Cancer*, **2019**, *18* (1), 110. https://doi.org/10.1186/s12943-019-1036-9.

[115] Tang, J.; Wang, F.; Cheng, G.; Si, S.; Sun, X.; Han, J.; Yu, H.; Zhang, W.; Lv, Q.; Wei, J.-F.; et al. Wilms' Tumor 1-Associating Protein Promotes Renal Cell Carcinoma Proliferation by Regulating CDK2 MRNA Stability. *J. Exp. Clin. Cancer Res.*, **2018**, *37* (1), 40. https://doi.org/10.1186/s13046-018-0706-6.

[116] Dahal, U.; Le, K.; Gupta, M. RNA M6A Methyltransferase METTL3 Regulates Invasiveness of Melanoma Cells by Matrix Metallopeptidase 2. *Melanoma Res.*, **2019**, *29* (4), 382–389. https://doi.org/10.1097/CMR.0000000000000580.

[117] Cui, Q.; Shi, H.; Ye, P.; Li, L.; Qu, Q.; Sun, G.; Sun, G.; Lu, Z.; Huang, Y.; Yang, C.-G.; et al. M6A RNA Methylation Regulates the Self-Renewal and Tumorigenesis of Glioblastoma Stem Cells. *Cell Rep.*, **2017**, *18* (11), 2622–2634. https://doi.org/10.1016/j.celrep.2017.02.059.

[118] Zhang, S.; Zhao, B. S.; Zhou, A.; Lin, K.; Zheng, S.; Lu, Z.; Chen, Y.; Sulman, E. P.; Xie, K.; Bögler, O.; et al. The M6A Demethylase ALKBH5 Maintains Tumorigenicity of Glioblastoma Stem-Like Cells by Sustaining FOXM1 Expression and Cell Proliferation Program. *Cancer Cell*, **2017**, *31* (4), 591-606.e6. https://doi.org/10.1016/j.ccell.2017.02.013.
[119] Zhang, C.; Samanta, D.; Lu, H.; Bullen, J. W.; Zhang, H.; Chen, I.; He, X.; Semenza, G. L. Hypoxia Induces the Breast Cancer Stem Cell Phenotype by HIF-Dependent and ALKBH5-Mediated M6A-Demethylation of NANOG MRNA. *Proc. Natl. Acad. Sci.*, **2016**, *113* (14), E2047–E2056. https://doi.org/10.1073/pnas.1602883113.
[120] Shen, C.; Sheng, Y.; Zhu, A. C.; Robinson, S.; Jiang, X.; Dong, L.; Chen, H.; Su, R.; Yin, Z.; Li, W.; et al. RNA Demethylase ALKBH5 Selectively Promotes Tumorigenesis and Cancer Stem Cell Self-Renewal in Acute Myeloid Leukemia. *Cell Stem Cell*, **2020**, *27* (1), 64–80.e9. https://doi.org/10.1016/j.stem.2020.04.009.
[121] Weng, H.; Huang, H.; Wu, H.; Qin, X.; Zhao, B. S.; Dong, L.; Shi, H.; Skibbe, J.; Shen, C.; Hu, C.; et al. METTL14 Inhibits Hematopoietic Stem/Progenitor Differentiation and Promotes Leukemogenesis via MRNA M6A Modification. *Cell Stem Cell*, **2018**, *22* (2), 191-205.e9. https://doi.org/10.1016/j.stem.2017.11.016.
[122] Berman, H. M.; Westbrook, J.; Feng, Z.; Gilliland, G.; Bhat, T. N.; Weissig, H.; Shindyalov, I. N.; Bourne, P. E. The Protein Data Bank. *Nucleic Acids Res.*, **2000**, *28* (1), 235–242. https://doi.org/10.1093/nar/28.1.235.
[123] Sastry, G. M.; Adzhigirey, M.; Day, T.; Annabhimoju, R.; Sherman, W. Protein and Ligand Preparation: Parameters, Protocols, and Influence on Virtual Screening Enrichments. *J. Comput. Aided Mol. Des.*, **2013**, *27* (3), 221–234. https://doi.org/10.1007/s10822-013-9644-8.
[124] Stephens, P. J.; Devlin, F. J.; Chabalowski, C. F.; Frisch, M. J. Ab Initio Calculation of Vibrational Absorption and Circular Dichroism Spectra Using Density Functional Force Fields. *J. Phys. Chem.*, **1994**, *98* (45), 11623–11627. https://doi.org/10.1021/j100096a001.
[125] Morris, G. M.; Huey, R.; Lindstrom, W.; Sanner, M. F.; Belew, R. K.; Goodsell, D. S.; Olson, A. J. AutoDock4 and AutoDockTools4: Automated Docking with Selective Receptor Flexibility. *J. Comput. Chem.*, **2009**, *30* (16), 2785–2791. https://doi.org/10.1002/jcc.21256.
[126] Schönbach, C.; Koh, J. L. Y.; Flower, D. R.; Wong, L.; Brusic, V. FIMM, a Database of Functional Molecular Immunology: Update 2002. *Nucleic Acids Res.*, **2002**, *30* (1), 226–229. https://doi.org/10.1093/nar/30.1.226.
[127] Schrödinger Release 2018-1: LigPrep, Schrödinger. LLC, New York, NY. 2018.
[128] Friesner, R. A.; Murphy, R. B.; Repasky, M. P.; Frye, L. L.; Greenwood, J. R.; Halgren, T. A.; Sanschagrin, P. C.; Mainz, D. T. Extra Precision Glide: Docking and Scoring Incorporating a Model of Hydrophobic Enclosure for Protein−Ligand Complexes. *J. Med. Chem.*, **2006**, *49* (21), 6177–6196. https://doi.org/10.1021/jm051256o.
[129] Halgren, T. A.; Murphy, R. B.; Friesner, R. A.; Beard, H. S.; Frye, L. L.; Pollard, W. T.; Banks, J. L. Glide: A New Approach for Rapid, Accurate Docking and Scoring. 2. Enrichment Factors in Database Screening. *J. Med. Chem.*, **2004**, *47* (7), 1750–1759. https://doi.org/10.1021/jm030644s.
[130] Jorgensen, W. L.; Tirado-Rives, J. The OPLS [Optimized Potentials for Liquid Simulations] Potential Functions for Proteins, Energy Minimizations for Crystals

of Cyclic Peptides and Crambin. *J. Am. Chem. Soc.*, **1988**, *110* (6), 1657–1666. https://doi.org/10.1021/ja00214a001.

[131] Jorgensen, W. L.; Maxwell, D. S.; Tirado-Rives, J. Development and Testing of the OPLS All-Atom Force Field on Conformational Energetics and Properties of Organic Liquids. *J. Am. Chem. Soc.*, **1996**, *118* (45), 11225–11236. https://doi.org/10.1021/ja9621760.

[132] Bowers, K. J.; Chow, D. E.; Xu, H.; Dror, R. O.; Eastwood, M. P.; Gregersen, B. A.; Klepeis, J. L.; Kolossvary, I.; Moraes, M. A.; Sacerdoti, F. D.; et al. Scalable Algorithms for Molecular Dynamics Simulations on Commodity Clusters. In *SC '06: Proceedings of the 2006 ACM/IEEE Conference on Supercomputing*; 2006; pp 43–43. https://doi.org/10.1109/SC.2006.54.

[133] Schrödinger Suite, Release 2018, Schrödinger. LLC, New York, NY. 2018.

[134] Li, F.; Kennedy, S.; Hajian, T.; Gibson, E.; Seitova, A.; Xu, C.; Arrowsmith, C. H.; Vedadi, M. A Radioactivity-Based Assay for Screening Human M6A-RNA Methyltransferase, METTL3-METTL14 Complex, and Demethylase ALKBH5. *J. Biomol. Screen.*, **2016**, *21* (3), 290–297. https://doi.org/10.1177/1087057115623264.

[135] Karlsson, R. Affinity Analysis of Non-Steady-State Data Obtained under Mass Transport Limited Conditions Using BIAcore Technology. *J. Mol. Recognit.*, **1999**, *12* (5), 285–292. https://doi.org/10.1002/(SICI)1099-1352(199909/10)12:5<285::AID-JMR469>3.0.CO;2-Y.

[136] Myszka, D. G.; He, X.; Dembo, M.; Morton, T. A.; Goldstein, B. Extending the Range of Rate Constants Available from BIACORE: Interpreting Mass Transport-Influenced Binding Data. *Biophys. J.*, **1998**, *75* (2), 583–594.

[137] Rich, R. L.; Myszka, D. G. Higher-Throughput, Label-Free, Real-Time Molecular Interaction Analysis. *Anal. Biochem.*, **2007**, *361* (1), 1–6. https://doi.org/10.1016/j.ab.2006.10.040.

[138] Asmari, M.; Ratih, R.; Alhazmi, H. A.; El Deeb, S. Thermophoresis for Characterizing Biomolecular Interaction. *Methods San Diego Calif*, **2018**, *146*, 107–119. https://doi.org/10.1016/j.ymeth.2018.02.003.

[139] Lomenick, B.; Hao, R.; Jonai, N.; Chin, R. M.; Aghajan, M.; Warburton, S.; Wang, J.; Wu, R. P.; Gomez, F.; Loo, J. A.; et al. Target Identification Using Drug Affinity Responsive Target Stability (DARTS). *Proc. Natl. Acad. Sci.*, **2009**, *106* (51), 21984–21989. https://doi.org/10.1073/pnas.0910040106.

[140] Pai, M. Y.; Lomenick, B.; Hwang, H.; Schiestl, R.; McBride, W.; Loo, J. A.; Huang, J. Drug Affinity Responsive Target Stability (DARTS) for Small Molecule Target Identification. *Methods Mol. Biol. Clifton NJ*, **2015**, *1263*, 287–298. https://doi.org/10.1007/978-1-4939-2269-7_22.

[141] Carpenter, A. E.; Jones, T. R.; Lamprecht, M. R.; Clarke, C.; Kang, I. H.; Friman, O.; Guertin, D. A.; Chang, J. H.; Lindquist, R. A.; Moffat, J.; et al. CellProfiler: Image Analysis Software for Identifying and Quantifying Cell Phenotypes. *Genome Biol.*, **2006**, *7* (10), R100. https://doi.org/10.1186/gb-2006-7-10-r100.

[142] Mahato, A. K.; Kopra, J.; Renko, J.-M.; Visnapuu, T.; Korhonen, I.; Pulkkinen, N.; Bespalov, M. M.; Domanskyi, A.; Ronken, E.; Piepponen, T. P.; et al. Glial Cell Line–Derived Neurotrophic Factor Receptor Rearranged During Transfection Agonist Supports Dopamine Neurons In Vitro and Enhances Dopamine Release In Vivo. *Mov. Disord.*, **2020**, *35* (2), 245–255. https://doi.org/10.1002/mds.27943.

[143] Liu, J.; Yue, Y.; He, C. Preparation of Human Nuclear RNA M6A Methyltransferases and Demethylases and Biochemical Characterization of Their Catalytic Activity. In *Methods in Enzymology*; He, C., Ed.; RNA Modification; Academic Press, 2015; Vol. 560, pp 117–130. https://doi.org/10.1016/bs.mie.2015.03.013.

[144] Irwin, J. J.; Shoichet, B. K. ZINC − A Free Database of Commercially Available Compounds for Virtual Screening. *J. Chem. Inf. Model.*, **2005**, *45* (1), 177–182. https://doi.org/10.1021/ci049714+.

[145] Law, V.; Knox, C.; Djoumbou, Y.; Jewison, T.; Guo, A. C.; Liu, Y.; Maciejewski, A.; Arndt, D.; Wilson, M.; Neveu, V.; et al. DrugBank 4.0: Shedding New Light on Drug Metabolism. *Nucleic Acids Res.*, **2014**, *42* (Database issue), D1091–D1097. https://doi.org/10.1093/nar/gkt1068.

[146] McMurray, F.; Demetriades, M.; Aik, W.; Merkestein, M.; Kramer, H.; Andrew, D. S.; Scudamore, C. L.; Hough, T. A.; Wells, S.; Ashcroft, F. M.; et al. Pharmacological Inhibition of FTO. *PLOS ONE*, **2015**, *10* (4), e0121829. https://doi.org/10.1371/journal.pone.0121829.

[147] Qiao, Y.; Zhou, B.; Zhang, M.; Liu, W.; Han, Z.; Song, C.; Yu, W.; Yang, Q.; Wang, R.; Wang, S.; et al. A Novel Inhibitor of the Obesity-Related Protein FTO. *Biochemistry*, **2016**, *55* (10), 1516–1522. https://doi.org/10.1021/acs.biochem.6b00023.

[148] Xu, C.; Wang, X.; Liu, K.; Roundtree, I. A.; Tempel, W.; Li, Y.; Lu, Z.; He, C.; Min, J. Structural Basis for Selective Binding of M6A RNA by the YTHDC1 YTH Domain. *Nat. Chem. Biol.*, **2014**, *10* (11), 927–929. https://doi.org/10.1038/nchembio.1654.

SUMMARY IN ESTONIAN

Epitranskriptoomiliste protsesside madalmolekulaarsete regulaatorite arendus

Antud väitekirja põhieesmärk oli leida uudseid ühendeid, mis võimaldaks modifitseerida RNA N^6-metüüladenosiini (m^6A) metüleerimist soovitud suunas, inhibeerides või aktiveerides RNA m^6A modifitseerimisega tegelevaid ensüüme. Ühendite leidmiseks kasutati molekulaarse modelleerimise meetodeid ning ühendit aktiivsust kontrolliti erinevate eksperimentaalsete meetoditega. Parimate ligandide toimet uuriti erinevate patoloogiate *in vitro* mudelites.

Väitekirjas esimeses osas kirjeldatakse RNA m^6A metüültransferaasi METTL3/METTL14/WTAP ensüümkompleksi madalmolekulaarsete aktivaatorite avastamist. Molekulaarsesildamise ning molekulaardünaamika simulatsioonide alusel leiti neli eriti kõrge sidumisafiinsusega ühendit, mis pinna plasma resonantsi (SPR) meetodiga mõõtes näitasid parimatel juhtudel valgule sidumise dissotsiatsioonikonstandi väärtuseid madalas nanomolaarses alas. Ensüümkatses mõõdetud EC_{50} väärtused näitasid, et ühendid aktiveerivad RNA metüleerimist METTL3/METTL14/WTAP ensüümkompleksi abil samuti nanomolaarsete kontsentratsioonide juures. Avastatud RNA m^6A metüleerimise aktivaatorite toimet uuriti HIV-1 viiruse replikatsioonile. Kõik aktivaatorid suurendasid viiruse replikatsiooni, kõige suurem mõju oli aktivaatoril **4I**. Antud ühend suurendas m^6A taset nii rakkude mRNAs kui ka viiruse RNAs.

Väitekirja teises osas keskenduti RNA m^6A demetülaasi FTO kirjanduses teadaolevate inhibiitorite struktuuri optimeerimisele, kasutades molekulaarse modelleerimise meetodeid. Ennustati kuus uut potentsiaalset inhibiitorit, millest kaks ühendit näitasid eksperimentaalsetes katsetes aktiivsust mikromolaarsel tasemel. Inhibeerimise kontsentratsiooni väärtused olid vastavalt IC_{50} = 1,46 μM ühendi **2II** puhul ja IC_{50} = 28,9 μM ühendi **3II** korral. Nende FTO inhibiitorite mõju testiti *in vitro* Parkinsoni haiguse mudelil, mis põhineb kasvufaktori hülgamisest tingitud närvirakkude apoptoosil. Mõlemad FTO inhibiitorid omasid silmapaistvalt tugevat neuroprotektiivset toimet juba madalate nanomolaarsete kontsentratsioonide korral.

Väitekirja kolmandas osas tegeleti RNA m^6A demetülaasi ALKBH5 uute inhibiitorite otsingutega. Inhibiitorite leidmiseks kasutati suure läbilaskevõimega virtuaalset sõelumist ning lisaks molekulaardünaamika simulatsioone. Kuuest parima arvutuslikult ennustatud sidumisafiinsusega molekulist omasid eksperimentaalkatsetes aktiivsust ühendid **3III** (IC_{50} = 0,84 μM) ja **6III** (IC_{50} = 1,79 μM). Kuna ALKBH5 ensüümi ekspressioon on tihedalt seotud erinevate vähivormide tekkega, siis vaadeldi leitud inhibiitorite mõju mitmetele leukeemia rakuliinidele. Mõlemad leitud ALKBH5 ensüümi inhibiitorid näitasid inhibeerivat toimet leukeemia rakuliinidele HL-60, CCRF-CEM ning K-562 madalate mikromolekulaarsete kontsentratsioonide korral.

Kokkuvõtteks, antud väitekirjas uuriti kolme RNA m^6A metüleerimisega seotud ensüümi. Kõigile uuritud ensüümidele leiti uued ligandid (aktivaatorid või inhibiitorid) aktiivsusega nanomolaarsete või madalate mikromolaarsete kontsentratsioonide piirkonnas. Antud ühendeid edasi optimeerides on võimalik saada uusi sobivaid ravimikanditaate erinevate patoloogiate vastu.

ACKNOWLEDGEMENTS

First, I would like to express my gratitude to Prof. Mati Karelson for the supervision, guidance, and support throughout all these years. I would like to thank Dr. Esko Kankuri, Prof. Mart Saarma and Prof. Andres Merits for their useful advice and constructive feedback. I am thankful to Dr. Eva Žusinaite for the help in biological experiments. Also, I would like to sincerely thank all co-authors of articles for their valuable contributions.

This work was supported by Chemestmed Ltd. (Tartu, Estonia) and Centre of Excellence in Molecular Cell Engineering, Estonia, 2014-2020.4.01.15-013.

PUBLICATIONS

CURRICULUM VITAE

Name: Simona Selberg
Date of birth: July 29, 1993, Kuressaare, Estonia
Citizenship: Estonia
Contact: Institute of Chemistry, University of Tartu, Ravila 14a, Tartu, 50411, Estonia
E-mail: simona.selberg@ut.ee

Education:

2017–...	University of Tartu, Institute of Chemistry, PhD student
2015–2017	University of Tartu, Institute of Chemistry, M.Sc. (Chemistry)
2012–2015	University of Tartu, Institute of Chemistry, B.Sc. (Chemistry)

Professional employment:

02.2017 – …	Chemist, University of Tartu, Institute of Chemistry

Scientific publications:

1. Selberg, S.; Blokhina, D.; Aatonen, M.; Koivisto, P.; Siltanen, A.; Mervaala, E.; Kankuri, E.; Karelson, M. Discovery of Small Molecules that Activate RNA Methylation through Cooperative Binding to the METTL3-14-WTAP Complex Active Site. *Cell Reports* **2019**, 26 (13), 3762–3771, DOI: 10.1016/j.celrep.2019.02.100.
2. Selberg, S.; Yu, L.-Y.; Bondarenko, O.; Kankuri, E.; Seli, N.; Kovaleva, V.; Herodes, K.; Saarma, M.; Karelson, M. Small-Molecule Inhibitors of the RNA m^6A Demethylases FTO Potently Support the Survival of Dopamine Neurons. *International Journal of Molecular Sciences* **2021**, 22 (9), 4537, DOI: 10.3390/ijms22094537.
3. Selberg, S.; Seli, N.; Kankuri, E.; Karelson, M. Rational Design of Novel Anticancer Small-Molecule RNA m6A Demethylase ALKBH5 Inhibitors. *ACS Omega* **2021**, 6 (20), 13310-13320, DOI: 10.1021/acsomega.1c01289.
4. Selberg, S.; Žusinaite, E.; Herodes, K.; Seli, N.; Kankuri, E.; Merits, A.; Karelson, M. HIV replication is increased by RNA methylation METTL3/ METTL14/WTAP complex activators. *ACS Omega* **2021**, 6 (24), 15957–15963, DOI: 10.1021/acsomega.1c01626.

Industrial property:

1. Selberg, S.; Blokhina, D.; Kankuri, E.; Karelson, M. A Method of Modulating the RNA Methylation, WO/2019/197024A1, 2019.
2. Selberg, S.; Žusinaite, E.; Merits, A.; Karelson, M. A Method of Modulating HIV-1 Provirus Activation and Replication, WO/2020/114583A1, 2020.
3. Selberg, S.; Karelson, M. A Method of Suppressing Cancer by RNA m^6A Demethylase ALKBH5 Inhibitors, WO/2020/207550A1, 2020.

Poster presentations:

1. Selberg, S.; Blokhina, D.; Aatonen, M.; Koivisto, P.; Siltanen, A.; Mervaala, E.; Kankuri, E.; Karelson, M. (2018). Discovery of RNA methyltransferase METTL3/14 small-molecule activators. Heidelberg, Germany, 25–27 April 2018.
2. Selberg, S.; Žusinaite, E.; Herodes, K.; Merits, A.; Karelson, M. (2019). Effect of RNA m^6A methyltransferase complex METTL3/METTL14/ WTAP small-molecule activators on HIV-1 virus replication. Frankfurt, Germany, 26–27 November 2019.

ELULOOKIRJELDUS

Nimi: Simona Selberg
Sünniaeg: 29. juuli 1993, Kuressaare, Eesti
Kodakondsus: Eesti
Kontakt: Tartu Ülikool keemia instituut, Ravila 14a, Tartu, 50411, Eesti
E-post: simona.selberg@ut.ee

Haridus:

2017–...	Tartu Ülikool, Keemia instituut, doktoriõpe (keemia)
2015–2017	Tartu Ülikool, Keemia instituut, magistriõpe (keemia)
2012–2015	Tartu Ülikool, Keemia instituut, bakalaureuseõpe (keemia)

Töökogemus:

02.2017–…	Tartu Ülikool, keemik

Teaduspublikatsioonid:

1. Selberg, S.; Blokhina, D.; Aatonen, M.; Koivisto, P.; Siltanen, A.; Mervaala, E.; Kankuri, E.; Karelson, M. Discovery of Small Molecules that Activate RNA Methylation through Cooperative Binding to the METTL3-14-WTAP Complex Active Site. *Cell Reports* **2019**, 26 (13), 3762–3771, DOI: 10.1016/j.celrep.2019.02.100.
2. Selberg, S.; Yu, L.-Y.; Bondarenko, O.; Kankuri, E.; Seli, N.; Kovaleva, V.; Herodes, K.; Saarma, M.; Karelson, M. Small-Molecule Inhibitors of the RNA m^6A Demethylases FTO Potently Support the Survival of Dopamine Neurons. *International Journal of Molecular Sciences* **2021**, 22 (9), 4537, DOI: 10.3390/ijms22094537.
3. Selberg, S.; Seli, N.; Kankuri, E.; Karelson, M. Rational Design of Novel Anticancer Small-Molecule RNA m6A Demethylase ALKBH5 Inhibitors. ACS *Omega* **2021**, 6 (20), 13310-13320, DOI: 10.1021/acsomega.1c01289.
4. Selberg, S.; Žusinaite, E.; Herodes, K.; Seli, N.; Kankuri, E.; Merits, A.; Karelson, M. HIV replication is increased by RNA methylation METTL3/ METTL14/WTAP complex activators. *ACS Omega* **2021**, 6 (24), 15957–15963, DOI: 10.1021/acsomega.1c01626.

Tööstusomand:

1. Selberg, S.; Blokhina, D.; Kankuri, E.; Karelson, M. A Method of Modulating the RNA Methylation, WO/2019/197024A1, 2019.
2. Selberg, S.; Žusinaite, E.; Merits, A.; Karelson, M. A Method of Modulating HIV-1 Provirus Activation and Replication, WO/2020/114583A1, 2020.
3. Selberg, S.; Karelson, M. A Method of Suppressing Cancer by RNA m^6A Demethylase ALKBH5 Inhibitors, WO/2020/207550A1, 2020.

Posterettekanded:

1. Selberg, S.; Blokhina, D.; Aatonen, M.; Koivisto, P.; Siltanen, A.; Mervaala, E.; Kankuri, E.; Karelson, M. (2018). Discovery of RNA methyltransferase METTL3/14 small-molecule activators. Heidelberg, Saksamaa, 25–27 aprill 2018.
2. Selberg, S.; Žusinaite, E.; Herodes, K.; Merits, A.; Karelson, M. (2019). Effect of RNA m^6A methyltransferase complex METTL3/METTL14/ WTAP small-molecule activators on HIV-1 virus replication. Frankfurt, Saksamaa, 26–27 november 2019.

DISSERTATIONES CHIMICAE UNIVERSITATIS TARTUENSIS

1. **Toomas Tamm.** Quantum-chemical simulation of solvent effects. Tartu, 1993, 110 p.
2. **Peeter Burk.** Theoretical study of gas-phase acid-base equilibria. Tartu, 1994, 96 p.
3. **Victor Lobanov.** Quantitative structure-property relationships in large descriptor spaces. Tartu, 1995, 135 p.
4. **Vahur Mäemets.** The ^{17}O and ^{1}H nuclear magnetic resonance study of H_2O in individual solvents and its charged clusters in aqueous solutions of electrolytes. Tartu, 1997, 140 p.
5. **Andrus Metsala.** Microcanonical rate constant in nonequilibrium distribution of vibrational energy and in restricted intramolecular vibrational energy redistribution on the basis of slater's theory of unimolecular reactions. Tartu, 1997, 150 p.
6. **Uko Maran.** Quantum-mechanical study of potential energy surfaces in different environments. Tartu, 1997, 137 p.
7. **Alar Jänes.** Adsorption of organic compounds on antimony, bismuth and cadmium electrodes. Tartu, 1998, 219 p.
8. **Kaido Tammeveski.** Oxygen electroreduction on thin platinum films and the electrochemical detection of superoxide anion. Tartu, 1998, 139 p.
9. **Ivo Leito.** Studies of Brønsted acid-base equilibria in water and non-aqueous media. Tartu, 1998, 101 p.
10. **Jaan Leis.** Conformational dynamics and equilibria in amides. Tartu, 1998, 131 p.
11. **Toonika Rinken.** The modelling of amperometric biosensors based on oxidoreductases. Tartu, 2000, 108 p.
12. **Dmitri Panov.** Partially solvated Grignard reagents. Tartu, 2000, 64 p.
13. **Kaja Orupõld.** Treatment and analysis of phenolic wastewater with microorganisms. Tartu, 2000, 123 p.
14. **Jüri Ivask.** Ion Chromatographic determination of major anions and cations in polar ice core. Tartu, 2000, 85 p.
15. **Lauri Vares.** Stereoselective Synthesis of Tetrahydrofuran and Tetrahydropyran Derivatives by Use of Asymmetric Horner-Wadsworth-Emmons and Ring Closure Reactions. Tartu, 2000, 184 p.
16. **Martin Lepiku.** Kinetic aspects of dopamine D_2 receptor interactions with specific ligands. Tartu, 2000, 81 p.
17. **Katrin Sak.** Some aspects of ligand specificity of P2Y receptors. Tartu, 2000, 106 p.
18. **Vello Pällin.** The role of solvation in the formation of iotsitch complexes. Tartu, 2001, 95 p.
19. **Katrin Kollist.** Interactions between polycyclic aromatic compounds and humic substances. Tartu, 2001, 93 p.

20. **Ivar Koppel.** Quantum chemical study of acidity of strong and superstrong Brønsted acids. Tartu, 2001, 104 p.
21. **Viljar Pihl.** The study of the substituent and solvent effects on the acidity of OH and CH acids. Tartu, 2001, 132 p.
22. **Natalia Palm.** Specification of the minimum, sufficient and significant set of descriptors for general description of solvent effects. Tartu, 2001, 134 p.
23. **Sulev Sild.** QSPR/QSAR approaches for complex molecular systems. Tartu, 2001, 134 p.
24. **Ruslan Petrukhin.** Industrial applications of the quantitative structure-property relationships. Tartu, 2001, 162 p.
25. **Boris V. Rogovoy.** Synthesis of (benzotriazolyl)carboximidamides and their application in relations with *N*- and *S*-nucleophyles. Tartu, 2002, 84 p.
26. **Koit Herodes.** Solvent effects on UV-vis absorption spectra of some solvatochromic substances in binary solvent mixtures: the preferential solvation model. Tartu, 2002, 102 p.
27. **Anti Perkson.** Synthesis and characterisation of nanostructured carbon. Tartu, 2002, 152 p.
28. **Ivari Kaljurand.** Self-consistent acidity scales of neutral and cationic Brønsted acids in acetonitrile and tetrahydrofuran. Tartu, 2003, 108 p.
29. **Karmen Lust.** Adsorption of anions on bismuth single crystal electrodes. Tartu, 2003, 128 p.
30. **Mare Piirsalu.** Substituent, temperature and solvent effects on the alkaline hydrolysis of substituted phenyl and alkyl esters of benzoic acid. Tartu, 2003, 156 p.
31. **Meeri Sassian.** Reactions of partially solvated Grignard reagents. Tartu, 2003, 78 p.
32. **Tarmo Tamm.** Quantum chemical modelling of polypyrrole. Tartu, 2003. 100 p.
33. **Erik Teinemaa.** The environmental fate of the particulate matter and organic pollutants from an oil shale power plant. Tartu, 2003. 102 p.
34. **Jaana Tammiku-Taul.** Quantum chemical study of the properties of Grignard reagents. Tartu, 2003. 120 p.
35. **Andre Lomaka.** Biomedical applications of predictive computational chemistry. Tartu, 2003. 132 p.
36. **Kostyantyn Kirichenko.** Benzotriazole – Mediated Carbon–Carbon Bond Formation. Tartu, 2003. 132 p.
37. **Gunnar Nurk.** Adsorption kinetics of some organic compounds on bismuth single crystal electrodes. Tartu, 2003, 170 p.
38. **Mati Arulepp.** Electrochemical characteristics of porous carbon materials and electrical double layer capacitors. Tartu, 2003, 196 p.
39. **Dan Cornel Fara.** QSPR modeling of complexation and distribution of organic compounds. Tartu, 2004, 126 p.
40. **Riina Mahlapuu.** Signalling of galanin and amyloid precursor protein through adenylate cyclase. Tartu, 2004, 124 p.

41. **Mihkel Kerikmäe.** Some luminescent materials for dosimetric applications and physical research. Tartu, 2004, 143 p.
42. **Jaanus Kruusma.** Determination of some important trace metal ions in human blood. Tartu, 2004, 115 p.
43. **Urmas Johanson.** Investigations of the electrochemical properties of polypyrrole modified electrodes. Tartu, 2004, 91 p.
44. **Kaido Sillar.** Computational study of the acid sites in zeolite ZSM-5. Tartu, 2004, 80 p.
45. **Aldo Oras.** Kinetic aspects of dATPαS interaction with $P2Y_1$ receptor. Tartu, 2004, 75 p.
46. **Erik Mölder.** Measurement of the oxygen mass transfer through the air-water interface. Tartu, 2005, 73 p.
47. **Thomas Thomberg.** The kinetics of electroreduction of peroxodisulfate anion on cadmium (0001) single crystal electrode. Tartu, 2005, 95 p.
48. **Olavi Loog.** Aspects of condensations of carbonyl compounds and their imine analogues. Tartu, 2005, 83 p.
49. **Siim Salmar.** Effect of ultrasound on ester hydrolysis in aqueous ethanol. Tartu, 2006, 73 p.
50. **Ain Uustare.** Modulation of signal transduction of heptahelical receptors by other receptors and G proteins. Tartu, 2006, 121 p.
51. **Sergei Yurchenko.** Determination of some carcinogenic contaminants in food. Tartu, 2006, 143 p.
52. **Kaido Tämm.** QSPR modeling of some properties of organic compounds. Tartu, 2006, 67 p.
53. **Olga Tšubrik.** New methods in the synthesis of multisubstituted hydrazines. Tartu. 2006, 183 p.
54. **Lilli Sooväli.** Spectrophotometric measurements and their uncertainty in chemical analysis and dissociation constant measurements. Tartu, 2006, 125 p.
55. **Eve Koort.** Uncertainty estimation of potentiometrically measured ph and pK_a values. Tartu, 2006, 139 p.
56. **Sergei Kopanchuk.** Regulation of ligand binding to melanocortin receptor subtypes. Tartu, 2006, 119 p.
57. **Silvar Kallip.** Surface structure of some bismuth and antimony single crystal electrodes. Tartu, 2006, 107 p.
58. **Kristjan Saal.** Surface silanization and its application in biomolecule coupling. Tartu, 2006, 77 p.
59. **Tanel Tätte.** High viscosity $Sn(OBu)_4$ oligomeric concentrates and their applications in technology. Tartu, 2006, 91 p.
60. **Dimitar Atanasov Dobchev**. Robust QSAR methods for the prediction of properties from molecular structure. Tartu, 2006, 118 p.
61. **Hannes Hagu**. Impact of ultrasound on hydrophobic interactions in solutions. Tartu, 2007, 81 p.
62. **Rutha Jäger.** Electroreduction of peroxodisulfate anion on bismuth electrodes. Tartu, 2007, 142 p.

63. **Kaido Viht.** Immobilizable bisubstrate-analogue inhibitors of basophilic protein kinases: development and application in biosensors. Tartu, 2007, 88 p.
64. **Eva-Ingrid Rõõm.** Acid-base equilibria in nonpolar media. Tartu, 2007, 156 p.
65. **Sven Tamp.** DFT study of the cesium cation containing complexes relevant to the cesium cation binding by the humic acids. Tartu, 2007, 102 p.
66. **Jaak Nerut.** Electroreduction of hexacyanoferrate(III) anion on Cadmium (0001) single crystal electrode. Tartu, 2007, 180 p.
67. **Lauri Jalukse.** Measurement uncertainty estimation in amperometric dissolved oxygen concentration measurement. Tartu, 2007, 112 p.
68. **Aime Lust.** Charge state of dopants and ordered clusters formation in CaF_2:Mn and CaF_2:Eu luminophors. Tartu, 2007, 100 p.
69. **Iiris Kahn**. Quantitative Structure-Activity Relationships of environmentally relevant properties. Tartu, 2007, 98 p.
70. **Mari Reinik.** Nitrates, nitrites, N-nitrosamines and polycyclic aromatic hydrocarbons in food: analytical methods, occurrence and dietary intake. Tartu, 2007, 172 p.
71. **Heili Kasuk.** Thermodynamic parameters and adsorption kinetics of organic compounds forming the compact adsorption layer at Bi single crystal electrodes. Tartu, 2007, 212 p.
72. **Erki Enkvist.** Synthesis of adenosine-peptide conjugates for biological applications. Tartu, 2007, 114 p.
73. **Svetoslav Hristov Slavov**. Biomedical applications of the QSAR approach. Tartu, 2007, 146 p.
74. **Eneli Härk.** Electroreduction of complex cations on electrochemically polished Bi(*hkl*) single crystal electrodes. Tartu, 2008, 158 p.
75. **Priit Möller.** Electrochemical characteristics of some cathodes for medium temperature solid oxide fuel cells, synthesized by solid state reaction technique. Tartu, 2008, 90 p.
76. **Signe Viggor.** Impact of biochemical parameters of genetically different pseudomonads at the degradation of phenolic compounds. Tartu, 2008, 122 p.
77. **Ave Sarapuu.** Electrochemical reduction of oxygen on quinone-modified carbon electrodes and on thin films of platinum and gold. Tartu, 2008, 134 p.
78. **Agnes Kütt.** Studies of acid-base equilibria in non-aqueous media. Tartu, 2008, 198 p.
79. **Rouvim Kadis.** Evaluation of measurement uncertainty in analytical chemistry: related concepts and some points of misinterpretation. Tartu, 2008, 118 p.
80. **Valter Reedo.** Elaboration of IVB group metal oxide structures and their possible applications. Tartu, 2008, 98 p.
81. **Aleksei Kuznetsov.** Allosteric effects in reactions catalyzed by the cAMP-dependent protein kinase catalytic subunit. Tartu, 2009, 133 p.

82. **Aleksei Bredihhin.** Use of mono- and polyanions in the synthesis of multisubstituted hydrazine derivatives. Tartu, 2009, 105 p.
83. **Anu Ploom.** Quantitative structure-reactivity analysis in organosilicon chemistry. Tartu, 2009, 99 p.
84. **Argo Vonk.** Determination of adenosine A_{2A}- and dopamine D_1 receptor-specific modulation of adenylate cyclase activity in rat striatum. Tartu, 2009, 129 p.
85. **Indrek Kivi.** Synthesis and electrochemical characterization of porous cathode materials for intermediate temperature solid oxide fuel cells. Tartu, 2009, 177 p.
86. **Jaanus Eskusson.** Synthesis and characterisation of diamond-like carbon thin films prepared by pulsed laser deposition method. Tartu, 2009, 117 p.
87. **Marko Lätt.** Carbide derived microporous carbon and electrical double layer capacitors. Tartu, 2009, 107 p.
88. **Vladimir Stepanov.** Slow conformational changes in dopamine transporter interaction with its ligands. Tartu, 2009, 103 p.
89. **Aleksander Trummal.** Computational Study of Structural and Solvent Effects on Acidities of Some Brønsted Acids. Tartu, 2009, 103 p.
90. **Eerold Vellemäe.** Applications of mischmetal in organic synthesis. Tartu, 2009, 93 p.
91. **Sven Parkel.** Ligand binding to 5-HT_{1A} receptors and its regulation by Mg^{2+} and Mn^{2+}. Tartu, 2010, 99 p.
92. **Signe Vahur.** Expanding the possibilities of ATR-FT-IR spectroscopy in determination of inorganic pigments. Tartu, 2010, 184 p.
93. **Tavo Romann**. Preparation and surface modification of bismuth thin film, porous, and microelectrodes. Tartu, 2010, 155 p.
94. **Nadežda Aleksejeva.** Electrocatalytic reduction of oxygen on carbon nanotube-based nanocomposite materials. Tartu, 2010, 147 p.
95. **Marko Kullapere.** Electrochemical properties of glassy carbon, nickel and gold electrodes modified with aryl groups. Tartu, 2010, 233 p.
96. **Liis Siinor.** Adsorption kinetics of ions at Bi single crystal planes from aqueous electrolyte solutions and room-temperature ionic liquids. Tartu, 2010, 101 p.
97. **Angela Vaasa.** Development of fluorescence-based kinetic and binding assays for characterization of protein kinases and their inhibitors. Tartu 2010, 101 p.
98. **Indrek Tulp.** Multivariate analysis of chemical and biological properties. Tartu 2010, 105 p.
99. **Aare Selberg.** Evaluation of environmental quality in Northern Estonia by the analysis of leachate. Tartu 2010, 117 p.
100. **Darja Lavõgina.** Development of protein kinase inhibitors based on adenosine analogue-oligoarginine conjugates. Tartu 2010, 248 p.
101. **Laura Herm.** Biochemistry of dopamine D_2 receptors and its association with motivated behaviour. Tartu 2010, 156 p.

102. **Terje Raudsepp.** Influence of dopant anions on the electrochemical properties of polypyrrole films. Tartu 2010, 112 p.
103. **Margus Marandi.** Electroformation of Polypyrrole Films: *In-situ* AFM and STM Study. Tartu 2011, 116 p.
104. **Kairi Kivirand.** Diamine oxidase-based biosensors: construction and working principles. Tartu, 2011, 140 p.
105. **Anneli Kruve.** Matrix effects in liquid-chromatography electrospray mass-spectrometry. Tartu, 2011, 156 p.
106. **Gary Urb.** Assessment of environmental impact of oil shale fly ash from PF and CFB combustion. Tartu, 2011, 108 p.
107. **Nikita Oskolkov.** A novel strategy for peptide-mediated cellular delivery and induction of endosomal escape. Tartu, 2011, 106 p.
108. **Dana Martin.** The QSPR/QSAR approach for the prediction of properties of fullerene derivatives. Tartu, 2011, 98 p.
109. **Säde Viirlaid.** Novel glutathione analogues and their antioxidant activity. Tartu, 2011, 106 p.
110. **Ülis Sõukand.** Simultaneous adsorption of Cd^{2+}, Ni^{2+}, and Pb^{2+} on peat. Tartu, 2011, 124 p.
111. **Lauri Lipping.** The acidity of strong and superstrong Brønsted acids, an outreach for the "limits of growth": a quantum chemical study. Tartu, 2011, 124 p.
112. **Heisi Kurig.** Electrical double-layer capacitors based on ionic liquids as electrolytes. Tartu, 2011, 146 p.
113. **Marje Kasari.** Bisubstrate luminescent probes, optical sensors and affinity adsorbents for measurement of active protein kinases in biological samples. Tartu, 2012, 126 p.
114. **Kalev Takkis.** Virtual screening of chemical databases for bioactive molecules. Tartu, 2012, 122 p.
115. **Ksenija Kisseljova**. Synthesis of aza-β^3-amino acid containing peptides and kinetic study of their phosphorylation by protein kinase A. Tartu, 2012, 104 p.
116. **Riin Rebane.** Advanced method development strategy for derivatization LC/ESI/MS. Tartu, 2012, 184 p.
117. **Vladislav Ivaništšev.** Double layer structure and adsorption kinetics of ions at metal electrodes in room temperature ionic liquids. Tartu, 2012, 128 p.
118. **Irja Helm.** High accuracy gravimetric Winkler method for determination of dissolved oxygen. Tartu, 2012, 139 p.
119. **Karin Kipper.** Fluoroalcohols as Components of LC-ESI-MS Eluents: Usage and Applications. Tartu, 2012, 164 p.
120. **Arno Ratas.** Energy storage and transfer in dosimetric luminescent materials. Tartu, 2012, 163 p.
121. **Reet Reinart-Okugbeni**. Assay systems for characterisation of subtype-selective binding and functional activity of ligands on dopamine receptors. Tartu, 2012, 159 p.

122. **Lauri Sikk.** Computational study of the Sonogashira cross-coupling reaction. Tartu, 2012, 81 p.
123. **Karita Raudkivi.** Neurochemical studies on inter-individual differences in affect-related behaviour of the laboratory rat. Tartu, 2012, 161 p.
124. **Indrek Saar.** Design of GalR2 subtype specific ligands: their role in depression-like behavior and feeding regulation. Tartu, 2013, 126 p.
125. **Ann Laheäär.** Electrochemical characterization of alkali metal salt based non-aqueous electrolytes for supercapacitors. Tartu, 2013, 127 p.
126. **Kerli Tõnurist.** Influence of electrospun separator materials properties on electrochemical performance of electrical double-layer capacitors. Tartu, 2013, 147 p.
127. **Kaija Põhako-Esko.** Novel organic and inorganic ionogels: preparation and characterization. Tartu, 2013, 124 p.
128. **Ivar Kruusenberg.** Electroreduction of oxygen on carbon nanomaterial-based catalysts. Tartu, 2013, 191 p.
129. **Sander Piiskop.** Kinetic effects of ultrasound in aqueous acetonitrile solutions. Tartu, 2013, 95 p.
130. **Ilona Faustova**. Regulatory role of L-type pyruvate kinase N-terminal domain. Tartu, 2013, 109 p.
131. **Kadi Tamm.** Synthesis and characterization of the micro-mesoporous anode materials and testing of the medium temperature solid oxide fuel cell single cells. Tartu, 2013, 138 p.
132. **Iva Bozhidarova Stoyanova-Slavova.** Validation of QSAR/QSPR for regulatory purposes. Tartu, 2013, 109 p.
133. **Vitali Grozovski**. Adsorption of organic molecules at single crystal electrodes studied by *in situ* STM method. Tartu, 2014, 146 p.
134. **Santa Veikšina**. Development of assay systems for characterisation of ligand binding properties to melanocortin 4 receptors. Tartu, 2014, 151 p.
135. **Jüri Liiv.** PVDF (polyvinylidene difluoride) as material for active element of twisting-ball displays. Tartu, 2014, 111 p.
136. **Kersti Vaarmets.** Electrochemical and physical characterization of pristine and activated molybdenum carbide-derived carbon electrodes for the oxygen electroreduction reaction. Tartu, 2014, 131 p.
137. **Lauri Tõntson**. Regulation of G-protein subtypes by receptors, guanine nucleotides and Mn^{2+}. Tartu, 2014, 105 p.
138. **Aiko Adamson.** Properties of amine-boranes and phosphorus analogues in the gas phase. Tartu, 2014, 78 p.
139. **Elo Kibena**. Electrochemical grafting of glassy carbon, gold, highly oriented pyrolytic graphite and chemical vapour deposition-grown graphene electrodes by diazonium reduction method. Tartu, 2014, 184 p.
140. **Teemu Näykki.** Novel Tools for Water Quality Monitoring – From Field to Laboratory. Tartu, 2014, 202 p.
141. **Karl Kaupmees.** Acidity and basicity in non-aqueous media: importance of solvent properties and purity. Tartu, 2014, 128 p.

142. **Oleg Lebedev**. Hydrazine polyanions: different strategies in the synthesis of heterocycles. Tartu, 2015, 118 p.
143. **Geven Piir.** Environmental risk assessment of chemicals using QSAR methods. Tartu, 2015, 123 p.
144. **Olga Mazina.** Development and application of the biosensor assay for measurements of cyclic adenosine monophosphate in studies of G protein-coupled receptor signalinga. Tartu, 2015, 116 p.
145. **Sandip Ashokrao Kadam.** Anion receptors: synthesis and accurate binding measurements. Tartu, 2015, 116 p.
146. **Indrek Tallo.** Synthesis and characterization of new micro-mesoporous carbide derived carbon materials for high energy and power density electrical double layer capacitors. Tartu, 2015, 148 p.
147. **Heiki Erikson.** Electrochemical reduction of oxygen on nanostructured palladium and gold catalysts. Tartu, 2015, 204 p.
148. **Erik Anderson.** *In situ* Scanning Tunnelling Microscopy studies of the interfacial structure between Bi(111) electrode and a room temperature ionic liquid. Tartu, 2015, 118 p.
149. **Girinath G. Pillai.** Computational Modelling of Diverse Chemical, Biochemical and Biomedical Properties. Tartu, 2015, 140 p.
150. **Piret Pikma.** Interfacial structure and adsorption of organic compounds at Cd(0001) and Sb(111) electrodes from ionic liquid and aqueous electrolytes: an *in situ* STM study. Tartu, 2015, 126 p.
151. **Ganesh babu Manoharan.** Combining chemical and genetic approaches for photoluminescence assays of protein kinases. Tartu, 2016, 126 p.
152. **Carolin Siimenson**. Electrochemical characterization of halide ion adsorption from liquid mixtures at Bi(111) and pyrolytic graphite electrode surface. Tartu, 2016, 110 p.
153. **Asko Laaniste.** Comparison and optimisation of novel mass spectrometry ionisation sources. Tartu, 2016, 156 p.
154. **Hanno Evard.** Estimating limit of detection for mass spectrometric analysis methods. Tartu, 2016, 224 p.
155. **Kadri Ligi.** Characterization and application of protein kinase-responsive organic probes with triplet-singlet energy transfer. Tartu, 2016, 122 p.
156. **Margarita Kagan.** Biosensing penicillins' residues in milk flows. Tartu, 2016, 130 p.
157. **Marie Kriisa.** Development of protein kinase-responsive photoluminescent probes and cellular regulators of protein phosphorylation. Tartu, 2016, 106 p.
158. **Mihkel Vestli.** Ultrasonic spray pyrolysis deposited electrolyte layers for intermediate temperature solid oxide fuel cells. Tartu, 2016, 156 p.
159. **Silver Sepp**. Influence of porosity of the carbide-derived carbon on the properties of the composite electrocatalysts and characteristics of polymer electrolyte fuel cells. Tartu, 2016, 137 p.
160. **Kristjan Haav**. Quantitative relative equilibrium constant measurements in supramolecular chemistry. Tartu, 2017, 158 p.

161. **Anu Teearu**. Development of MALDI-FT-ICR-MS methodology for the analysis of resinous materials. Tartu, 2017, 205 p.
162. **Taavi Ivan**. Bifunctional inhibitors and photoluminescent probes for studies on protein complexes. Tartu, 2017, 140 p.
163. **Maarja-Liisa Oldekop**. Characterization of amino acid derivatization reagents for LC-MS analysis. Tartu, 2017, 147 p.
164. **Kristel Jukk**. Electrochemical reduction of oxygen on platinum- and palladium-based nanocatalysts. Tartu, 2017, 250 p.
165. **Siim Kukk**. Kinetic aspects of interaction between dopamine transporter and *N*-substituted nortropane derivatives. Tartu, 2017, 107 p.
166. **Birgit Viira**. Design and modelling in early drug development in targeting HIV-1 reverse transcriptase and Malaria. Tartu, 2017, 172 p.
167. **Rait Kivi**. Allostery in cAMP dependent protein kinase catalytic subunit. Tartu, 2017, 115 p.
168. **Agnes Heering**. Experimental realization and applications of the unified acidity scale. Tartu, 2017, 123 p.
169. **Delia Juronen**. Biosensing system for the rapid multiplex detection of mastitis-causing pathogens in milk. Tartu, 2018, 85 p.
170. **Hedi Rahnel.** ARC-inhibitors: from reliable biochemical assays to regulators of physiology of cells. Tartu, 2018, 176 p.
171. **Anton Ruzanov.** Computational investigation of the electrical double layer at metal–aqueous solution and metal–ionic liquid interfaces. Tartu, 2018, 129 p.
172. **Katrin Kestav.** Crystal Structure-Guided Development of Bisubstrate-Analogue Inhibitors of Mitotic Protein Kinase Haspin. Tartu, 2018, 166 p.
173. **Mihkel Ilisson.** Synthesis of novel heterocyclic hydrazine derivatives and their conjugates. Tartu, 2018, 101 p.
174. **Anni Allikalt.** Development of assay systems for studying ligand binding to dopamine receptors. Tartu, 2018, 160 p.
175. **Ove Oll.** Electrical double layer structure and energy storage characteristics of ionic liquid based capacitors. Tartu, 2018, 187 p.
176. **Rasmus Palm.** Carbon materials for energy storage applications. Tartu, 2018, 114 p.
177. **Jörgen Metsik.** Preparation and stability of poly(3,4-ethylenedioxythiophene) thin films for transparent electrode applications. Tartu, 2018, 111 p.
178. **Sofja Tšepelevitš.** Experimental studies and modeling of solute-solvent interactions. Tartu, 2018, 109 p.
179. **Märt Lõkov.** Basicity of some nitrogen, phosphorus and carbon bases in acetonitrile. Tartu, 2018, 104 p.
180. **Anton Mastitski**. Preparation of α-aza-amino acid precursors and related compounds by novel methods of reductive one-pot alkylation and direct alkylation. Tartu, 2018, 155 p.
181. **Jürgen Vahter**. Development of bisubstrate inhibitors for protein kinase CK2. Tartu, 2019, 186 p.

182. **Piia Liigand.** Expanding and improving methodology and applications of ionization efficiency measurements. Tartu, 2019, 189 p.
183. **Sigrid Selberg.** Synthesis and properties of lipophilic phosphazene-based indicator molecules. Tartu, 2019, 74 p.
184. **Jaanus Liigand.** Standard substance free quantification for LC/ESI/MS analysis based on the predicted ionization efficiencies. Tartu, 2019, 254 p.
185. **Marek Mooste.** Surface and electrochemical characterisation of aryl film and nanocomposite material modified carbon and metal-based electrodes. Tartu, 2019, 304 p.
186. **Mare Oja.** Experimental investigation and modelling of pH profiles for effective membrane permeability of drug substances. Tartu, 2019, 306 p.
187. **Sajid Hussain.** Electrochemical reduction of oxygen on supported Pt catalysts. Tartu, 2019, 220 p.
188. **Ronald Väli.** Glucose-derived hard carbon electrode materials for sodium-ion batteries. Tartu, 2019, 180 p.
189. **Ester Tee.** Analysis and development of selective synthesis methods of hierarchical micro- and mesoporous carbons. Tartu, 2019, 210 p.
190. **Martin Maide.** Influence of the microstructure and chemical composition of the fuel electrode on the electrochemical performance of reversible solid oxide fuel cell. Tartu, 2020, 144 p.
191. **Edith Viirlaid.** Biosensing Pesticides in Water Samples. Tartu, 2020, 102 p.
192. **Maike Käärik.** Nanoporous carbon: the controlled nanostructure, and structure-property relationships. Tartu, 2020, 162 p.
193. **Artur Gornischeff.** Study of ionization efficiencies for derivatized compounds in LC/ESI/MS and their application for targeted analysis. Tartu, 2020, 124 p.
194. **Reet Link.** Ligand binding, allosteric modulation and constitutive activity of melanocortin-4 receptors. Tartu, 2020, 108 p.
195. **Pilleriin Peets.** Development of instrumental methods for the analysis of textile fibres and dyes. Tartu, 2020, 150 p.
196. **Larisa Ivanova.** Design of active compounds against neurodegenerative diseases. Tartu, 2020, 152 p.
197. **Meelis Härmas.** Impact of activated carbon microstructure and porosity on electrochemical performance of electrical double-layer capacitors. Tartu, 2020, 122 p.
198. **Ruta Hecht.** Novel Eluent Additives for LC-MS Based Bioanalytical Methods. Tartu, 2020, 202 p.
199. **Max Hecht.** Advances in the Development of a Point-of-Care Mass Spectrometer Test. Tartu, 2020, 168 p.
200. **Ida Rahu.** Bromine formation in inorganic bromide/nitrate mixtures and its application for oxidative aromatic bromination. Tartu, 2020, 116 p.
201. **Sander Ratso**. Electrocatalysis of oxygen reduction on non-precious metal catalysts. Tartu, 2020, 371 p.
202. **Astrid Darnell.** Computational design of anion receptors and evaluation of host-guest binding. Tartu, 2021, 150 p.

203. **Ove Korjus.** The development of ceramic fuel electrode for solid oxide cells. Tartu, 2021, 150 p.
204. **Merit Oss.** Ionization efficiency in electrospray ionization source and its relations to compounds' physico-chemical properties. Tartu, 2021, 124 p.
205. **Madis Lüsi**. Electroreduction of oxygen on nanostructured palladium catalysts. Tartu, 2021, 180 p.
206. **Eliise Tammekivi.** Derivatization and quantitative gas-chromatographic analysis of oils. Tartu, 2021, 122 p.